Published in final edited form as:
Prog Brain Res. 2010 ; 187: 111–136. doi:10.1016/B978-0-444-53613-6.00008-3.

Synaptically Activated Burst-Generating Conductances Underlie a Group-Pacemaker Mechanism for Respiratory Rhythm Generation in Mammals

Christopher A. Del Negro[1], **John A. Hayes**[1,§], **Ryland W. Pace**[1], **Benjamin R. Brush**[1], **Ryoichi Teruyama**[3], and **Jack L. Feldman**[2]

[1]Department of Applied Science, McGlothlin-Street Hall, The College of William & Mary, Williamsburg, Virginia, USA. Ryland W. Pace Tel: 757-645-8904, rylandpace@gmail.com. Benjamin R. Brush Tel: 774-278-0645, brbrus@gmail.com

[2]Department of Neurobiology, David Geffen School of Medicine, University of California at Los Angeles, Los Angeles, California, USA. Tel: 310-825-0954, Fax: 310-825-2224, feldman@ucla.edu

[3]Department of Biological Sciences, Louisiana State University, Baton Rouge, Louisiana, USA. Tel: 225-578-4623, Fax: 225-578-2597, rteruyama@lsu.edu

Abstract

Breathing, chewing and walking are critical life-sustaining behaviors in mammals that consist essentially of simple rhythmic movements. Breathing movements in particular involve the diaphragm, thorax, and airways but emanate from a network in the lower brain stem. This network can be studied in reduced preparations *in vitro* and using simplified mathematical models that make testable predictions. An iterative approach that employs both *in vitro* and *in silico* models has ruled out canonical mechanisms for respiratory rhythm that involve *reciprocal inhibition* and *pacemaker properties*. We present an alternative model in which emergent network properties play the key rhythmogenic role. Specifically, we show evidence that synaptically activated burst-generating conductances – which are only available in the context of network activity – engender robust periodic bursts in respiratory neurons. Because the cellular burst-generating mechanism is linked to network synaptic drive we dub this type of system a *group pacemaker*.

Keywords

preBötzinger Complex; pre-Bötzinger Complex; central pattern generator (CPG); metabotropic glutamate receptors; calcium-activated nonspecific cation current; mathematical models; emergent network properties; breathing

INTRODUCTION

Understanding the neural origins of behaviors like walking, running, swimming, chewing, suckling, and breathing will be tenable via the application of a broad spectrum of techniques from biomechanics to molecular genetics. These cross-disciplinary tools will enable us to

Correspondence: Christopher A. Del Negro, Ph.D., Associate Professor of Applied Science, McGlothlin-Street Hall, Room 318, The College of William & Mary, Williamsburg, Virginia 23187-8795, USA, 757-221-7808 (office), 757-221-7749 (lab), 757-221-2050 (fax), cadeln@wm.edu.
[§]Present address: Neurobiologie & Développement, Institut de Neurobiologie Alfred Fessard, Centre National de la Recherche Scientifique, Gif sur Yvette cedex, France. Tel: +33 (0) 1 69 82 34 55, Fax: +33 (0) 1 69 82 41 78, john.hayes@inaf.cnrs-gif.fr.

cohere data from many levels of analysis spanning intact behaving organisms to intrinsic membrane properties and biochemical signaling pathways studied *in vitro*.

Here we examine breathing behavior in mammals: rhythmic movements of the diaphragm, thorax, and airways to produce ventilation. We seek cellular- and synaptic-level mechanisms that produce the respiratory rhythm. We limit our focus to a specialized region of the lower brain stem (preBötzinger Complex; preBötC), which is essential for breathing in awake intact adult rodents, and is necessary and sufficient for inspiratory motor rhythms *in vitro* (Smith et al., 1991, Rekling and Feldman, 1998, Feldman and Del Negro, 2006).

To focus on the neural origins of the essential underlying inspiratory rhythm we necessarily set aside other, equally important, issues related to the neural control of breathing, including – but not limited to – the developmental genetics of preBötC circuits, integrated functions of the preBötC within the larger respiratory network of the lower medulla, formation of an appropriate spatiotemporal motor pattern for ventilatory movements, regulation of the rhythm via neuromodulation, sensorimotor integration, e.g., mechanosensitive feedback from the lungs, as well as peripheral and central chemosensation related to oxygen, carbon dioxide, and pH.

Our analysis of rhythm generation in the preBötC addresses two linked questions: i) *Which neurons?* ii) *How*? The preBötC is a functionally and anatomically defined site in the lower brain stem containing several thousand neurons in rodents, and we are interested in understanding which ones are rhythmogenic. Here, we consider intrinsic membrane and anatomical properties that may underlie rhythmogenicity.

Several models – conceptual as well as explicitly mathematical –outline two general paradigms for the mechanism underlying respiratory rhythmogenesis: *reciprocal inhibition and/*or *pacemaker neurons*. Here we evaluate some straightforward predictions of these models and conclude that the respiratory rhythm cannot be adequately explained using these paradigms. Instead we present an alternative model: *group-pacemaker hypothesis* (Rekling et al., 1996a, Rekling and Feldman, 1998, Feldman and Del Negro, 2006, Rubin et al., 2009a). In this model, recurrent synaptic excitation boosts and propagates activity like a conventional network oscillator (Grillner, 2006), yet constituent neurons generate spike bursts with an underlying plateau-like depolarization during the active phase, which is behavior typically associated with intrinsic pacemaker properties (Coombes and Bressloff, 2005).

RHYTHMIC MOTOR BEHAVIORS STUDIED *IN VITRO*

Central pattern generator (CPG) networks produce neural rhythms for motor behaviors without need of sensory feedback or commands from higher brain centers (Marder, 2001, Grillner, 2006). Invertebrate model systems provide valuable insights into the structure and function of CPGs because these systems comprise a limited number of constituent neurons (~10–<100) that can be identified and, more importantly, selectively recorded in the context of behavior *in vitro*. Detailed analyses of CPG neurons and their intrinsic and synaptic properties have led to mathematical models that reconstitute the behaving system *in silico*. Explicit models make testable predictions to complement experimental data. This engenders an iterative process in which models are created from empirical measurements, and refined by testing their predictions, which ultimately leads to critical experiments (particularly, *in vivo*) that advance understanding about the neural underpinnings of these behaviors (Fig. 1A).

Unraveling CPGs in mammalian systems including spinal locomotor networks as well as hindbrain oral-motor and respiratory oscillators is considerably more difficult. Mammalian

CPGs are composed of far more neurons (>1000), and with some notable exceptions, function, e.g., rhythm generation, may be anatomically dispersed. Moreover, basic morphological or even intrinsic features may not be sufficient to classify neurons and impute their function. To discern the identity of a neuron and analyze its function in the CPG, we must consider a host of challenging approaches to measure properties, such as transmitter phenotype, projection patterns, i.e., synaptic connectivity, morphology, and intrinsic membrane properties as they relate to influencing burst generation and rhythmic activity. Regarding intrinsic neuronal properties, there is no substitute at present for intracellular recordings in the context of fictive behavior *in vitro*.

Molecular genetics has been enormously useful in defining and testing the roles of specific classes of spinal interneurons (Goulding and Pfaff, 2005, Goulding, 2009), which can then be isolated and studied in reduced *in vitro* preparations (Hinckley et al., 2005, Wilson et al., 2005, Gosgnach et al., 2006, Hinckley and Ziskind-Conhaim, 2006, Wilson et al., 2007, Dyck and Gosgnach, 2009, Dougherty and Kiehn, 2010, Wilson et al., 2010, Zhong et al., 2010). However, despite profound breakthroughs in defining and understanding the composition of spinal locomotor circuits that produce left-right alternation and enforce rhythmic stability, finding the core of the CPG – that is, elucidating its rhythmogenic constituents – has remained elusive (Brownstone and Wilson, 2008, Kiehn et al., 2008).

The oral-motor CPG has also been isolated and studied *in vitro* in neonatal rats. Recordings can be obtained from the motor branch of the trigeminal nerve or, in preparations where the mandible is left attached, rhythmic jaw movements can be monitored *in situ* (Kogo et al., 1996, Tanaka et al., 1999). The rhythmogenic circuits appear to be located within the lateral reticular formation at the level of the trigeminal motor nucleus. An interesting neuronal phenotype that develops intrinsic bursting behavior in response to decreasing levels of extracellular Ca^{2+} has been identified in the trigeminal sensory nucleus (Brocard et al., 2006, Kolta et al., 2007). Whether these neurons function as rhythm-generators for fictive behavior *in vitro* or during oral-motor behaviors *in vivo* remains a compelling notion to be tested.

The respiratory CPG is particularly advantageous with regard to defining the putative rhythm-generating neurons at the core of a CPG. First, inspiratory rhythmogenic circuits are contained in the preBötC (Smith et al., 1991, Gray et al., 1999, Guyenet and Wang, 2001, Wang et al., 2001, Guyenet et al., 2002, Stornetta et al., 2003). Second, inspiratory rhythms must be fully developed at birth to then function unceasingly in support of life-sustaining breathing movements. The combination of these factors yields a robust system that fortuitously can be reliably reduced to 300–500 μm thick transverse slice preparations from neonatal rodents that isolate the preBötC and can spontaneously generate respiratory-related rhythmic motor nerve output from the hypoglossal (XII) nerve (Fig. 1B,C). Slices provide optimal experimental access to the constituent rhythmogenic neurons for imaging and electrophysiology in the transverse plane, in the context of behaviorally relevant network functions. The slice preparation serves as a reliable and convenient *in vitro* experimental model widely used since 1991 by numerous laboratories. Discoveries in the slice have consistently motivated new models of rhythm generation, e.g., (Butera et al., 1999a, Butera et al., 1999b, Del Negro et al., 2001, Kosmidis et al., 2004, Smith et al., 2007, Rubin et al., 2009a) and lead to novel tests in behaving animals (Gray et al., 2001, Wenninger et al., 2004a, Wenninger et al., 2004b, McKay et al., 2005, Tan et al., 2008).

ROLE OF PACEMAKER PROPERTIES IN RESPIRATORY RHYTHMOGENESIS

Early models featured a role for chloride-mediated synaptic inhibition

Prior to 1989 the dominant models of respiratory rhythm generation incorporated a critical and obligatory role for synaptic inhibition (Bradley et al., 1975, Feldman and Cowan, 1975). The general structure of these models posited (a minimum of) three interconnected populations of respiratory neurons including inspiratory and expiratory timing circuits, as well as well as a ramp-generator circuit for inspiratory bursts. The interaction of these populations was thought to generate two or three distinct phases of the respiratory cycle *in vivo*: inspiration, and expiration, which some models divided into stage 1 expiration, i.e., the post-inspiratory phase, and stage 2 expiration. Inhibitory synaptic interactions were postulated to account for the following aspects of the respiratory cycle: 1) Regulation of the augmenting ramp of inspiratory activity via recurrent inhibition, which serves as a check against runaway recurrent excitation and linearized inspiration. 2) Termination of inspiratory bursts via a transient surge of inhibition. 3) Promotion of a phase transition from stage 1 to stage 2 expiration via synaptic inhibition between post-inspiratory (post-I) neurons and the augmenting-expiratory (aug-E) neurons that become active in stage 2. 4) Assure mutually exclusive activity patterns between inspiratory and expiratory neurons through reciprocal inhibition (for a thorough review, see: Feldman, 1986).

This general model was in many ways the respiratory analog of that originally proposed by T.G. Brown for locomotion, in which two opposing phases of a motor pattern could be generated by reciprocal inhibition of the ‘half centers’ (Brown, 1911, Brown, 1914). In the respiratory cycle, however, inhibitory interactions were further postulated to underlie the additional functions.

However, when put to the test using the brain stem-spinal cord preparation *in vitro*, respiratory rhythm continued unabated after the removal of chloride-mediated synaptic inhibition (Feldman and Smith, 1989). This fundamental result, has been extensively replicated using a variety of pharmacological and ion substitution methods in a variety of experimental systems including the *en bloc* brain stem-spinal cord preparation and the slice preparation from neonatal rats and mice, in turtle *en bloc* preparations, and in the working heart-brainstem preparation from adult mice (Shao and Feldman, 1997, Brockhaus and Ballanyi, 1998, Gray et al., 1999, Ritter and Zhang, 2000, Büsselberg et al., 2001, Johnson et al., 2002, Ren and Greer, 2006). Ionotropic synaptic inhibition contributes to normal breathing patterns *in vivo* (Richter and Spyer, 2001, Büsselberg et al., 2003) and influences the respiratory pattern formed by the brain stem circuits in which the preBötC is embedded (Smith et al., 2007, Rubin et al., 2009b) but it is not necessary for generating the fundamental rhythm *in vitro*, and thus is not an essential feature of the respiratory CPG in the preBötC (Feldman and Del Negro, 2006).

Neurons with oscillatory bursting properties become integrated into models of rhythmogenesis

The original report that proposed the preBötC as a site of respiratory rhythmogenesis (Smith et al., 1991) identified a subset of inspiratory neurons with voltage-dependent pacemaker properties, and suggested that such neurons could be rhythmogenic. Some preBötC inspiratory neurons, when depolarized with bias current, generate ectopic bursts in the interburst interval, i.e., between XII motor discharges. After blocking excitatory synaptic interactions, these same neurons continue to burst rhythmically, as long as baseline membrane potential remains sufficiently depolarized. A thorough search using unit and whole-cell recordings *in vitro* reveals inspiratory (both excitatory and inhibitory, Morgado-

Valle et al., 2010), expiratory, and non-respiratory (tonic) neurons with intrinsic bursting properties after synaptic isolation via low Ca^{2+} / high Mg^{2+} Ringer solution. Respiratory-modulated and -non-modulated neurons with bursting properties are widely distributed throughout the ventral medulla, including a region coextensive with the preBötC (Johnson et al., 1994). These results are consistent with the originally speculative notion that intrinsic oscillatory bursting neurons could be the source of respiratory rhythm (Feldman and Cleland, 1982).

We refer to *neurons with pacemaker properties* rather than *pacemaker neurons* because bursting in the absence of synaptic transmission has not been established in any way to constitute a distinct classification based on expression of intrinsic conductances, transmitter phenotype, or developmental lineage. The proposal that neurons with voltage-dependent bursting properties are rhythmogenic, i.e., the *pacemaker hypothesis*, became widely accepted without significant tests or proof. In part, the idea of pacemaker-driven CPG was a logical extension of principles well established in invertebrate systems, and the key prediction of the pacemaker hypothesis had been validated, namely that a subset of neurons with bursting-pacemaker properties are found within the preBötC (Smith et al., 1991, Johnson et al., 1994).

Butera and colleagues (1999b, 1999a) proposed a concrete mathematical model, which they dubbed a *hybrid pacemaker-network* (Smith et al., 1995) because it addressed the role of excitatory synaptic interactions in shaping rhythmic activity. Nevertheless, the pacemaker fraction of the network plays an obligatory role in the production of respiratory rhythm, unless the synaptic conductance was raised to unphysiological extremes (Butera et al., 1999b). The constituent neurons were assembled from a limited complement of ionophores, including persistent Na^+ current (I_{NaP}) and leakage K^+ current ($I_{K\text{-}Leak}$). These two intrinsic properties are distributed heterogeneously; the proper balance of g_{NaP} and $g_{K\text{-}Leak}$ endowed voltage-dependent pacemaker properties. Figure 2 plots g_{NaP} versus $g_{K\text{-}Leak}$ in the Butera model. Pacemaker behavior is expressed by neurons whose g_{NaP} and $g_{K\text{-}Leak}$ values are within the grey wedge in the center of the distribution. Within this wedge, the neurons express enough g_{NaP} to give 'burstiness' combined with low enough $g_{K\text{-}Leak}$ to ensure that the baseline membrane potential is depolarized within the voltage-dependent activation range for I_{NaP}. Neurons with g_{NaP} and $g_{K\text{-}Leak}$ outside this wedge region are either silent (black, lower right) or tonically spiking (white, upper left) (Fig. 2). For neurons in the silent or tonic states, applied current could offset the intrinsic $g_{K\text{-}Leak}$ and shift the cell behavior into the bursting regime (Butera et al., 1999a). Experimental data have been superimposed on the g_{NaP}-$g_{K\text{-}Leak}$ plot in Fig. 2. These points are paired measurements g_{NaP} and $g_{K\text{-}Leak}$ obtained from neurons with and without pacemaker properties in the neonatal rat preBötC. This demonstrates that a fraction of neurons with voltage-dependent bursting properties in the absence of synaptic transmission is a natural byproduct of heterogeneity.

The role of I_{NaP} was originally based on the observation of bursting in low Ca^{2+} solution (Johnson et al., 1994), and the role of $I_{K\text{-}Leak}$ was a straightforward prediction based on voltage-dependence of burst frequency. These ionic mechanisms for bursting have since been documented repeatedly (Smith et al., 1991, Koshiya and Smith, 1999, Del Negro et al., 2001, Del Negro et al., 2002a, Rybak et al., 2003, Koizumi and Smith, 2008, Koizumi et al., 2010). In 2001, Thoby-Brisson and Ramirez (2001) recognized, however, that bursting activity in synaptically isolated neurons could have another ionic basis, one that was sensitive to blockade by Cd^{2+}. We now know that this bursting mechanism involves the Ca^{2+}-activated nonspecific cationic current (I_{CAN}) (Pena et al., 2004, Del Negro et al., 2005). Although I_{CAN} is expressed throughout the perinatal period in ~96% of neurons in the preBötC, the number of neurons with I_{CAN}-mediated bursting properties after synaptic isolation is miniscule prior to P8 (0.6%), but can be as high as 8% after P8 (Pena et al.,

2004, Del Negro et al., 2005, Pace et al., 2007a). Throughout postnatal development the fraction of preBötC with voltage-dependent pacemaker properties attributable to g_{NaP}/g_{K}-Leak is between 5–25% (Pena et al., 2004, Del Negro et al., 2005, Pagliardini et al., 2005).

Evaluating the role of pacemaker properties in rhythm generation

Direct tests of whether bursting pacemaker activity is obligatory for rhythm generation came with use of the anticonvulsant drug riluzole (RIL) used, for some years, to treat amyotrophic lateral sclerosis. The therapeutic potential of RIL seemed attributable to both its ability to depress excitatory transmission (and thus prevent excitotoxicity), as well as its ability to decrease neural excitability through effects on Na^+ channels, I_{NaP} in particular (Doble, 1996). Applying RIL in the preBötC for the first time, we showed that RIL selectively attenuated I_{NaP} with a half-maximal effective concentration of ~3 μM, but had little effect on action potentials at concentrations less than 100 μM (Fig. 3). These effects matched those of RIL in neocortex (Urbani and Belluzzi, 2000) and were consistent for all preBötC neurons, not just neurons with bursting properties. RIL also hyperpolarized preBötC neurons by up to 5 mV by blocking the fraction of I_{NaP} open at baseline membrane potential, which typically is between −45 and −55 mV in the rhythmic slice preparation (Del Negro et al., 2002b). These effects of RIL on I_{NaP} in the preBötC and throughout the ventral medulla are now well established (Ptak et al., 2005, Koizumi and Smith, 2008).

Most important from the perspective of testing the pacemaker hypothesis, RIL completely precludes voltage-dependent bursting in synaptically isolated preBötC neurons (Fig. 4A). As to its effects on network activity, bath application of RIL at concentrations 1–200 μM has no effect on the frequency of respiratory rhythm in slice preparations from P0–4 neonatal rats and mice, in which I_{CAN} pacemaker activity is ostensibly nonexistent (Del Negro et al., 2002b). However, even while the frequency remained stable, longer exposure to RIL diminishes XII motor output, and causes the rhythmic signal *in vitro* to become undetectable (Del Negro et al., 2005) (Fig. 5A). The decrease in XII motor output occurs more slowly than the time required to block I_{NaP} and can be accounted for by decreases in cell excitability as well as the depression of excitatory transmission (Doble, 1996, Del Negro et al., 2005, Pace et al., 2007b). Nevertheless, to resolve whether the respiratory network could still function after blocking bursting-pacemaker activity, we performed three important follow-up experiments.

We repeated the experiment in P0–4 mice using 20-nM tetrodotoxin (TTX), which like RIL, fully blocks I_{NaP}. Bath application of 20 nM TTX to rhythmically active slices causes a time-dependent decrease in the XII motor output accompanied by a decrease in respiratory frequency. Prolonged exposure to 20-nM TTX stops rhythmic activity in slices (Fig. 5B). However, these experiments could not be unambiguously interpreted because 20 nM TTX (unlike RIL) also attenuated action potentials in preBötC neurons (Del Negro et al., 2005).

Even though the number of neurons with I_{CAN}-mediated bursting properties is vanishingly small P0–P4, we repeated the RIL experiments in rhythmically active slices in the presence of 100-μM flufenamic acid (FFA) (Fig. 6). This dose of FFA completely blocks I_{CAN}-mediated pacemaker activity (Fig. 4B) even though it does not block ICAN completely (Del Negro et al., 2005, Pace et al., 2007a). Interestingly, whether the rhythm stops by 20 nM TTX or the RIL + FFA cocktail, 0.5–2 μM of the excitatory neuropeptide Substance P (SP) or 0.5 μM of α-amino-3-hydroxy-5-methyl-4-isoxazole propionic acid (AMPA) is sufficient to revive it (Figs. 5B and 6). Neither SP nor AMPA induce a region of negative slope resistance in the steady-state current-voltage curve of preBötC neurons (Gray et al., 1999, Pena and Ramirez, 2004, Hayes and Del Negro, 2007) and thus cannot restore voltage-dependent bursting-pacemaker activity to neurons whose pacemaker-like activity has been precluded by RIL or low doses of TTX. The recovery of respiratory network rhythmicity

after pharmacological blockade of pacemaker activity strongly suggests RIL and low doses of TTX diminish respiratory motor output by attenuating excitability, rather than blocking pacemaker activity.

Finally, we injected RIL directly into the preBötC to selectively affect the rhythmogenic circuitry and avoid effects in other parts of the slice such as premotor and motor neurons, as well as neurons in the Raphé that provide serotonergic and peptidergic input to the preBötC (Ptak et al., 2009). Microinjection pipettes were targeted to the preBötC bilaterally and connected to a pressure source (400–600 mm Hg) gated by TTL pulses. With this system we apply RIL with very short duration repetitive pulses (8 ms at 3 Hz) while visualizing preBötC neurons under videomicroscopy to ensure that microinjection did not damage the tissue. With both microinjection pipettes properly positioned in the preBötC bilaterally, RIL microinjection for 20–40 min fails to perturb either the amplitude or frequency of respiratory rhythm (Pace et al., 2007b) (Fig. 7, lower trace). This fundamental result is the same when 100 μM FFA is present to preclude I_{CAN}-mediated pacemaker activity. As a control, to ensure that our protocol was effective for drug delivery, we microinjected the $GABA_A$ agonist muscimol, which rapidly stops respiratory rhythm (Fig. 7, upper traces). However, when either the left or right microinjection pipette is displaced, the unilateral microinjection of muscimol fails to impact rhythmogenesis (Pace et al., 2007b).

Koizumi and Smith (2008) also performed bilateral microinjection of RIL using thin slice preparations from neonatal rats. However, their protocol was slightly different and causes dose-dependent attenuation of respiratory frequency. One possible explanation for the disparity in the results is that Koizumi and Smith used thinner slices (~300 μm), which are more susceptible to decreases in excitability, which invariably accompanies RIL application. Another explanation is that Koizumi and Smith used continuous low-pressure infusion (10–20 mm Hg). This could create a channel in the tissue and direct the drug to the midline Raphé neurons, which play a critical role by delivering serotonin and SP to maintain excitability in the preBötC (Ptak et al., 2009). In fact, we tested this notion by targeting our microinjection pipettes to the Raphé in rhythmically active mouse slices and found that RIL microinjection to the Raphé bilaterally stop the respiratory rhythm in a few minutes (Pace et al., 2007b) (Fig. 8). The experiments recounted above suggest that bursting-pacemaker activity, whether its ionic mechanism depends on voltage-dependent I_{NaP} or I_{CAN}, is not obligatory for respiratory rhythm generation.

ROLE OF SYNAPTICALLY TRIGGERED BURST-GENERATING CONDUCTANCES IN RESPIRATORY RHYTHMOGENESIS

preBötC neurons with early-inspiratory activity and robust bursts may be rhythmogenic

If pacemaker properties after synaptic isolation are not necessarily a reliable and accurate phenotype for putative respiratory rhythm generators, then one should examine how respiratory neurons behave and, what intrinsic properties they utilize in the context of the functioning network, to elucidate the mechanisms of rhythmogenesis. This type of analysis is possible using slice preparations that retain the preBötC *in vitro* (Fig. 1B,C). An important pioneering work in that regard was the 1996 report by Rekling and colleagues which classified respiratory neurons in the preBötC and adjacent regions of the ventrolateral medulla according to several criteria including *inspiratory drive latency*, which quantifies the interval during which neurons depolarize and start to discharge spikes prior to the upstroke of XII motor output (Rekling et al., 1996a) (see Fig. 9). Neurons with the earliest inspiratory drive latency also had the highest input resistance, showed a ramp-like depolarization during the expiratory phase, and consistently achieved inspiratory burst amplitudes of 10–20 mV. In fact these inspiratory bursts were so strong that intraburst

depolarization block of spiking activity was common (see Fig. 9). When these same neurons were hyperpolarized using bias current to preclude spiking altogether, the inspiratory drive potential, denuded of spikes, was substantially identical in amplitude and duration to the envelope of the burst at normal baseline membrane potential with spiking present. This latter point suggested that the drive potential was triggered by synaptic activity and was not primarily attributable to voltage-dependent intrinsic currents (such as I_{NaP}, for example). Moreover, whole-cell recordings with the intracellular Na+ channel antagonist QX-314 in the patch solution did not diminish the drive potential amplitude, nor duration, which is further confirmation that inspiratory bursts are not primarily I_{NaP}-mediated (Pace et al., 2007b). Neurons with the above properties were suggested to be most closely involved in rhythm generation because they were the first subset of respiratory neurons to activate, i.e., earliest burst latency; their inspiratory bursts were robust, strong, and synaptically triggered; and finally their membrane properties were sensitive to modulation by neuropeptides that also modulated the respiratory period (Rekling et al., 1996b, Rekling et al., 1996a). Gray and colleagues (1999) then showed that peptide receptor expression, the neurokinin-1 receptor (NK1R) in particular, delineates the borders of the preBötC and that peptidergic modulation of the rhythm is a potential indicator for rhythmogenic neurons. Suzue recognized the modulatory effects of SP as early as 1984, but did not extend his analyses to the cellular, rhythmogenic level (Suzue, 1984). When NK1R-expressing ($NK1R^+$) neurons are destroyed in awake behaving rats using substance P (SP)-conjugated saporin toxin, normal breathing is abolished and the rats are left with an unphysiological ataxic respiratory pathology (Gray et al., 2001, McKay et al., 2005). Based on these studies *in vitro* and *in vivo*, the $NK1R^+$ subpopulation became an important putative rhythm-generating subset within the preBötC.

The $NK1R^+$ marker is imperfect, however. Some $NK1R^+$ neurons in the preBötC, particularly in the caudal region are substantially larger neurons with bulbospinal projections suggesting their function is likely of a premotor, not rhythmogenic, nature (Guyenet et al., 2002, Stornetta et al., 2003). When we began to label $NK1R^+$ neurons using a fluorescent tagging approach *in vitro* (Pagliardini et al., 2005, Hayes and Del Negro, 2007) we also found that $NK1R^+$ neurons are divisible according to size, quantified by whole-cell capacitance (C_M). The histogram of CM is bimodal (Fig. 9), which suggests that $NK1R^+$ neurons in the preBötC can be subdivided according to size. Neurons with larger C_M (~85 pF) could represent the bulbospinal premotor neurons, whereas the smaller C_M (~45 pF) neurons are more likely to represent the putative rhythm generators. These ~45 pF neurons are far more numerous, as shown by the histogram in Fig. 9, and also show significantly longer inspiratory drive latency (~250 ms), consistent with Rekling's original description (~300 ms). We dubbed this subset of small neurons *early inspiratory* to avoid confusion with the phenotype called *pre-inspiratory* by Onimaru and colleagues (Ballanyi et al., 1999), which are more rostrally located in a different respiratory nucleus, not the preBötC (Onimaru et al., 2008, Onimaru et al., 2009). These ~45 pF, early inspiratory preBötC neurons also show robust inspiratory bursts in which the underlying amplitude of the drive potential is 10–20 mV and depolarization block of intraburst spiking is common (Fig. 9, right), which suggests a strong and synaptically linked mechanism for inspiratory burst generation and was consistent with a rhythmogenic role in preBötC network function.

Calcium-activated nonspecific cation current triggered by excitatory synaptic input

We recorded early inspiratory neurons to dissect the synaptic and intrinsic factors of inspiratory burst generation. Using patch clamp to record in the whole-cell configuration, we added drugs to the patch solution that would block signaling pathways or intrinsic properties upon whole-cell dialysis. In that way we could measure the inspiratory burst prior to drug application via a perforated patch, and then, after rupturing the membrane with suction,

apply the drug from the cytoplasmic side to perturb the synaptic-intrinsic burst-generating mechanism, while leaving the entire network, other than the cell we recorded, pharmacologically unperturbed.

The large magnitude inspiratory bursts with intraburst depolarization block of spiking, which are shown schematically in Fig. 9, share some similarities with synaptically triggered plateau potentials that can have Ca^{2+} or Ca^{2+}-dependent ionic mechanisms. Therefore, we applied 30 mM K_4-BAPTA in the patch solution, which caused significant attenuation of the inspiratory burst and underlying drive potential (Fig. 10). When we subsequently added 100 μM FFA to the bath, there was no further reduction in the drive potential, which suggests that the inspiratory burst is mediated by I_{CAN} (Pace et al., 2007a). We also evoke I_{CAN} directly by adding the photolyzable Ca^{2+} chelator DM-nitrophen to the patch solution and expose the recorded soma and proximal dendrites to flashes of ultraviolet light (1–2 s). I_{CAN} reverses at ~0 mV, which is expected for a nonspecific cationic current (Fig. 11). Plateau-like bursts can also be evoked with current pulses after whole-cell dialysis with Cs^+, which enabled us to evoke I_{CAN} and evaluate its ionic basis using ion substitution (choline for Na^+) and test its Ca^{2+} activation mechanism by blocking voltage-dependent Ca^{2+} channels with 200 μM Cd^{2+} (Pace et al., 2007a). Either choline or Cd^{2+} is able to fully block I_{CAN}-mediated evoked plateaus. However, 100 μM FFA is an incomplete I_{CAN} blocker. In the presence of 100 μM FFA, some I_{CAN}-mediated plateau response could still be evoked by current pulse, and choline substitution is able to block the remaining response fully (Pace et al., 2007a).

Given the pharmacological limitations of 100 μM FFA, the fact that this dose of the drug did not stop respiratory rhythm *in vitro* was not a dispositive result (see Fig. 6). However, raising the concentration to 300–350 μM FFA fully blocked I_{CAN}-mediated evoked plateaus and, furthermore, stopped the respiratory rhythm. Once stopped, the respiratory rhythm could not be restarted using 1–2 μM SP (Pace et al., 2007a) (Fig. 12). This experiment strongly suggests that I_{CAN} is an essential cellular mechanism for rhythmogenesis. Nevertheless, concentrations of FFA exceeding 100 μM produce side effects that make interpretation of the results problematic (Teulon, 2000, Pace et al., 2007a).

The ion channels that underlie I_{CAN} are not known, but a potentially attractive set of candidates come from the *transient receptor potential* (TRP) family (Ramsey et al., 2006). In particular, TRPM4 and TRPM5 are unique because they are activated by Ca^{2+} but selective in their permeability for monovalent cations (Launay et al., 2002, Hofmann et al., 2003). We detected mRNA for TRPM4 and TRPM5 in preBötC tissues (Crowder et al., 2007) (Fig. 13A). The expression of TRPM4 and TRPM5 was tested using commercial antibodies from Santa Cruz Biotechnologies (Santa Cruz, CA) in adult rodent slice preparations (Fig. 13B). This resulted in heavy staining in preBötC and the neighboring nucleus ambiguous (NA). We additionally showed that I_{CAN}-mediated inspiratory drive potentials were labile to modulation of membrane phospholipids, notably phosphatidylinositol 4,5-bisphosphate (Crowder et al., 2007), which is characteristic behavior for TRPM4 and TRPM5 (Liu and Liman, 2003, Zhang et al., 2005). However, the molecular identity of I_{CAN} is by no means a solved problem. TRPM4 and TRPM5 are likely candidates, but other TRP channels including those from the canonical TRPC subfamily may be involved as well.

The experiments above showed that I_{CAN} played a substantial role in generating inspiratory bursts in the context of network activity. However, the synaptic activation mechanism was still unclear. It has been well established since the early 1990's that AMPA-type ionotropic glutamate receptors are critical for respiratory rhythm and that *N*-methyl-D-aspartate (NMDA) receptors are normally present but not essential for rhythmogenesis (Greer et al., 1991, Funk et al., 1993, Funk et al., 1997, Ge and Feldman, 1998, Morgado-Valle and

Feldman, 2007). If NMDA receptors were not the source of Ca^{2+} influx to activate I_{CAN} then it seemed possible that AMPA receptors could be Ca^{2+} permeable, despite anatomical evidence that AMPA receptors in the preBötC contain edited GluR2 subunits (Paarmann et al., 2000). We tested this physiologically by recording isolated preBötC neurons in the presence of 1 μM TTX. Short-duration pressure applications, i.e., puffs, of 500 nM AMPA caused a transient depolarization as a model of excitatory synaptic drive. Puffs were applied to the dendrite (~100 μm) to target the region likely to contain synapses and to avoid dislodging the patch-recording pipette at the soma. The AMPA puff response was completely blocked by GYKI 53655 (1-(4-aminophenyl)-4-methyl-7,8-methylenedioxy-5H-2,3-benzodiazepine), but could not be blocked using the selective antagonist for Ca^{2+}-permeable AMPA receptors IEM-1460 (N,N,N,-Trimethyl-5-[(tricyclo[3.3.1.13,7]dec-1-ylmethyl) amino]-1-pentanaminiumbromide hydrobromide) but, surprisingly, the response could be reduced by 70–75% by either FFA or Cd^{2+}, which indicated that the AMPA receptor was coupled to I_{CAN} activation, but not directly (Fig. 14). The coupling relies on local synaptic depolarization by AMPA receptors to evoke voltage-gated Ca^{2+} channels (Pace and Del Negro, 2008).

We also tested the role of metabotropic glutamate receptors (mGluRs) because group I mGluRs are coupled via phospholipase C (PLC) to the synthesis of inositol 1,4,5-trisphosphate (IP_3), which evokes intracellular Ca^{2+} release and could be a source of I_{CAN} activation. Approximately 40% of the inspiratory drive potential can be attributed to mGluR5, one of the two mGluR subtypes that comprise group I. The mGluR5-mediated component of the inspiratory drive potential was due to intracellular Ca^{2+} release causing I_{CAN} activation, as confirmed by intracellular blockade of IP_3 receptors by xestospongin (Fig. 15). The other member, mGluR1, was coupled to transient closure of K^+ channels in preBötC neurons, which also contributed to drive potential generation, but not via I_{CAN} (Pace et al., 2007b, Pace et al., 2007a).

GROUP PACEMAKER HYPOTHESIS OF RESPIRATORY RHYTHM GENERATION

A new paradigm for respiratory rhythmogenesis based on emergent network properties

In the absence of obligatory pacemaker neurons, one alternative explanation for rhythm generation is based on recurrent synaptic excitation. This concept remained purely hypothetical without the identification of specific mechanisms through which it could be implemented. However, we now recognize that I_{CAN} activation is linked to mGluRs and AMPA receptor-mediated recruitment of Ca^{2+} channels, which is a viable mechanism for the normally latent I_{CAN} to be evoked synaptically in the lead-up to inspiration (Pace et al., 2007a, Mironov, 2008).

Guided by experimental results, we assembled a mathematical model of a network with synaptically activated burst-generating conductances, which was dubbed a *group pacemaker* by Rekling and colleagues (Rekling et al., 1996a, Rekling and Feldman, 1998). Putatively rhythmogenic early-inspiratory neurons, e.g., Fig. 9 left, show ramp-like depolarization and low-rate spiking prior to the inspiratory phase, which is evidence of recurrent excitation (Rekling et al., 1996a, Rekling et al., 2000, Pace, 2007, Hartelt et al., 2008). There is significant depolarization block during the inspiratory burst, which produces a scoop-like attenuation of spike amplitude as the burst progresses. A transient period of quiescence follows burst termination, before the next cycle of recurrent excitation begins and synaptic depolarization and low-rate spiking restarts (Del Negro et al., 2009). These characteristic behaviors are visible during on-cell recording, as well as after whole-cell dialysis (Fig. 16A), and are recapped in the model (Fig. 16B) (Rubin et al., 2009a).

Constituent neurons in the group pacemaker model are not required to have pacemaker properties; that is, they need not exhibit rhythmic bursting without synaptic interactions. Low-rate spontaneous spiking activity in a subset of neurons engenders positive feedback via recurrent excitation. Glutamate causes postsynaptic depolarization via ionotropic AMPA receptors, and acts at mGluRs, which results in intracellular Ca^{2+} elevations that evoke I_{CAN}. Postsynaptic I_{CAN} contributes to burst generation by providing the plateau-like envelope of depolarization that makes up the inspiratory drive potential. I_{CAN} also helps terminate the burst. Intraburst spike attenuation, due to I_{CAN}-mediated depolarization block, diminishes recurrent excitation by causing a net reduction in transmitter release. Attenuated spikes in the model decrease excitatory synaptic drive by failing to reach a voltage-dependent threshold for release (Dobrunz et al., 1997, Forsythe et al., 1998, Brody and Yue, 2000), but physiological mechanisms include depletion of releasable vesicle pools or retrograde signaling that acts pre-synaptically to decrease release probability (Kettunen et al., 2005, Best and Regehr, 2008, Gibson et al., 2008). This sets the stage for burst termination by halting Ca^{2+} accumulation and deactivating I_{CAN}. Also, because Na^+ is the predominant charge carrier for inward I_{CAN}, intraburst Na^+ accumulation triggers activity-dependent outward currents such as the electrogenic Na^+/K^+ ATPase pump (I_{pump}) (Del Negro et al., 2009), Na^+-dependent K^+ current ($I_{K\text{-}Na}$), and ATP-dependent K^+ current ($I_{K\text{-}ATP}$, which activates as the ATPase pumps consume and thus diminish the available cytosolic ATP). I_{pump} is the main activity dependent current featured in detailed analyses of the model, but a wide array of activity dependent outward currents can accomplish the same basic burst-terminating function (Rubin et al., 2009a). Contrary to conventional wisdom (Hille, 2001), Ca^{2+}-dependent K^+ currents play no significant role in terminating inspiratory bursts (Onimaru et al., 2003, Crowder et al., 2007, Zavala-Tecuapetla et al., 2008). The Na^+-dependent outward currents actively hyperpolarize constituent neurons, leading to a transient quiescent state in the network. After a recovery period, sporadic spiking activity in the preBötC rekindles excitatory interconnections and restarts the cycle.

Figure 16 illustrates how network activity leads to an increase in intracellular Ca^{2+}, which subsequently evokes I_{CAN}. In turn, I_{CAN} causes Na^+ accumulation to evoke I_{pump} and other outward currents to cause burst termination. In the model system, this cycle can be visualized in the Na^+-Ca^{2+} phase plane and its underlying dynamics can be analyzed geometrically (Rinzel and Ermentrout, 1998).

Recurrent excitation and activity-dependent outward currents are well-established neurophysiological factors that influence cell and network activity. However, our CPG model depends on glutamatergic signaling to gate postsynaptic burst-generating ion channels. We further propose that short-term synaptic disfacilitation may also contribute to burst termination. This mechanism reflects a new paradigm for central pattern generation in which the rhythmogenic unit is the ensemble of pre- and postsynaptic features and can be properly considered a group pacemaker (Rekling et al., 1996a, Rekling and Feldman, 1998, Feldman and Del Negro, 2006).

This model is undoubtedly oversimplified, in that the individual neuron components are limited to single compartments in which synaptic integration and spike generation both takes place. This may not be an accurate depiction of burst generation in preBötC or in any CPG interneuron where significant processing depends on active dendrites (Stuart et al., 2007). However, the present model has the advantage of simplicity and tractability for mathematical analysis and can be readily assembled in networks.

CONCLUSIONS

CPGs in vertebrates incorporate thousands of highly interconnected neurons, each of which represents a complex dynamical system with many degrees of freedom (Grillner, 2006, Kozlov et al., 2009). To understand CPGs, we must necessarily focus on the essential rhythmogenic modules. Reciprocal inhibition – where active synaptic inhibition acts as a barrier that must be overcome for phase switching to occur – or specialized pacemaker neurons – which provide a rhythmic template for network activity – are modules that encapsulate rhythmic function in particular synaptic, i.e., inhibitory, or cellular properties (i.e., auto-oscillatory neurons with pacemaker, properties). Both mechanisms find widespread support in real systems. (Marder and Calabrese, 1996, Stein et al., 1997, Marder and Bucher, 2001, Grillner, 2006), but neither mechanism can explain preBötC rhythms (Feldman and Del Negro, 2006, Johnson et al., 2007, Pace et al., 2007a, Mironov, 2008, Morgado-Valle et al., 2010). The next level of module complexity would combine specific synaptic and cellular components, such as the synaptically activated burst-generating conductances that we propose underlie preBötC rhythmicity.

In CPG systems that depend on an active phase of inhibition or pacemaker properties, we speculate that synaptically activated burst-generating conductances may also be present, which could contribute to enhancing the robustness or duration of the active phase. Such a synaptically triggered conductance would be a convenient target for neuromodulation because its contribution could be modified to regulate the burst-phase without necessarily modifying the frequency or overall pattern of the motor rhythm.

Within the preBötC a synaptically activated burst-generating conductance appears to be important in conveying both the frequency and overall pattern of rhythmic activity. Yet there are many aspects of respiratory rhythm generation that are still not well understood. The group-pacemaker framework offers many directions for future tests to answer these questions using *in silico* models and a robust network with preserved function *in vitro*. Consequently, the principles brought to light may advance our understanding of the neural control of breathing and provide some insights into the neural origins of other motor behaviors as well.

Acknowledgments

The work was supported by NIH HL-40959, NIH NINDS R21 NS070056-01, NIHNHLBS R01 HL104127-01, and the Undergraduate Biological Sciences Education and Research Training Grant to The College of William & Mary by the Howard Hughes Memorial Institute.

REFERENCES

Ballanyi K, Onimaru H, Homma I. Respiratory network function in the isolated brainstem-spinal cord of newborn rats. Prog Neurobiol. 1999; 59:583–634. [PubMed: 10845755]

Best AR, Regehr WG. Serotonin evokes endocannabinoid release and retrogradely suppresses excitatory synapses. J Neurosci. 2008; 28:6508–6515. [PubMed: 18562622]

Bradley GW, Von Euler C, Marttila I, Roos B. A model of the central and reflex inhibition of inspiration in the cat. Biol Cybern. 1975; 19:105–116. [PubMed: 1191720]

Brocard F, Verdier D, Arsenault I, Lund JP, Kolta A. Emergence of intrinsic bursting in trigeminal sensory neurons parallels the acquisition of mastication in weanling rats. J Neurophysiol. 2006; 96:2410–2424. [PubMed: 16914618]

Brockhaus J, Ballanyi K. Synaptic inhibition in the isolated respiratory network of neonatal rats. Eur J Neurosci. 1998; 10:3823–3839. [PubMed: 9875360]

Brody DL, Yue DT. Release-independent short-term synaptic depression in cultured hippocampal neurons. J Neurosci. 2000; 20:2480–2494. [PubMed: 10729328]

Brown T. The intrinsic factors in the act of progression in the mammal. Proc R Soc Lond B. 1911; 84:308–319.

Brown TG. On the nature of the fundamental activity of the nervous centres: together with an analysis of the conditioning of rhythmic activity in progression, and a theory of the evolution of function in the nervous system. J Physiol. 1914; 48:18–46. [PubMed: 16993247]

Brownstone RM, Wilson JM. Strategies for delineating spinal locomotor rhythm-generating networks and the possible role of Hb9 interneurones in rhythmogenesis. Brain Res Rev. 2008; 57:64–76. [PubMed: 17905441]

Büsselberg D, Bischoff AM, Paton JF, Richter DW. Reorganisation of respiratory network activity after loss of glycinergic inhibition. Pflugers Arch. 2001; 441:444–449. [PubMed: 11212206]

Büsselberg D, Bischoff AM, Richter DW. A combined blockade of glycine and calcium-dependent potassium channels abolishes the respiratory rhythm. Neuroscience. 2003; 122:831–841. [PubMed: 14622925]

Butera RJ Jr, Rinzel J, Smith JC. Models of respiratory rhythm generation in the pre-Botzinger complex. I. Bursting pacemaker neurons. J Neurophysiol. 1999a; 82:382–397. [PubMed: 10400966]

Butera RJ Jr, Rinzel J, Smith JC. Models of respiratory rhythm generation in the pre-Botzinger complex. II. Populations Of coupled pacemaker neurons. J Neurophysiol. 1999b; 82:398–415. [PubMed: 10400967]

Coombes, S.; Bressloff, PC. Bursting : the genesis of rhythm in the nervous system. Hackensack, NJ: World Scientific Pub; 2005.

Crowder EA, Saha MS, Pace RW, Zhang H, Prestwich GD, Del Negro CA. Phosphatidylinositol 4,5-bisphosphate regulates inspiratory burst activity in the neonatal mouse preBotzinger complex. J Physiol. 2007; 582:1047–1058. [PubMed: 17599963]

Del Negro CA, Johnson SM, Butera RJ, Smith JC. Models of respiratory rhythm generation in the pre-Botzinger complex. III. Experimental tests of model predictions. J Neurophysiol. 2001; 86:59–74. [PubMed: 11431488]

Del Negro CA, Kam K, Hayes JA, Feldman JL. Asymmetric control of inspiratory and expiratory phases by excitability in the respiratory network of neonatal mice in vitro. J Physiol. 2009; 587:1217–1231. [PubMed: 19171658]

Del Negro CA, Koshiya N, Butera RJ Jr, Smith JC. Persistent sodium current, membrane properties and bursting behavior of pre-Bötzinger complex inspiratory neurons in vitro. J Neurophysiol. 2002a; 88:2242–2250. [PubMed: 12424266]

Del Negro CA, Morgado-Valle C, Feldman JL. Respiratory rhythm: an emergent network property? Neuron. 2002b; 34:821–830. [PubMed: 12062027]

Del Negro CA, Morgado-Valle C, Hayes JA, Mackay DD, Pace RW, Crowder EA, Feldman JL. Sodium and calcium current-mediated pacemaker neurons and respiratory rhythm generation. J Neurosci. 2005; 25:446–453. [PubMed: 15647488]

Doble A. The pharmacology and mechanism of action of riluzole. Neurology. 1996; 47:S233–S241. [PubMed: 8959995]

Dobrunz LE, Huang EP, Stevens CF. Very short-term plasticity in hippocampal synapses. Proc Natl Acad Sci U S A. 1997; 94:14843–14847. [PubMed: 9405701]

Dougherty KJ, Kiehn O. Firing and cellular properties of V2a interneurons in the rodent spinal cord. J Neurosci. 2010; 30:24–37. [PubMed: 20053884]

Dyck J, Gosgnach S. Whole cell recordings from visualized neurons in the inner laminae of the functionally intact spinal cord. J Neurophysiol. 2009; 102:590–597. [PubMed: 19386756]

Feldman, JL. Neurophysiology of breathing in mammals. In: Bloom, FE., editor. Handbook of Physiology; Section I: The Nervous System; Volume IV: Intrinsic Regulatory Systems of the Brain. Bethesda, MD: Am. Physiol. Soc.; 1986.

Feldman, JL.; Cleland, C. Possible roles of pacemaker neurons in mammalian respiratory rhythmogenesis. In: Carpenter, D., editor. Cellular Pacemakers. New York: Wiley; 1982.

Feldman JL, Cowan JD. Large-scale activity in neural nets II: A model for the brainstem respiratory oscillator. Biol Cybern. 1975; 17:39–51. [PubMed: 1115819]

Feldman JL, Del Negro CA. Looking for inspiration: new perspectives on respiratory rhythm. Nat Rev Neurosci. 2006; 7:232–242. [PubMed: 16495944]

Feldman JL, Smith JC. Cellular mechanisms underlying modulation of breathing pattern in mammals. Ann N Y Acad Sci. 1989; 563:114–130. [PubMed: 2476055]

Forsythe ID, Tsujimoto T, Barnes-Davies M, Cuttle MF, Takahashi T. Inactivation of presynaptic calcium current contributes to synaptic depression at a fast central synapse. Neuron. 1998; 20:797–807. [PubMed: 9581770]

Funk GD, Johnson SM, Smith JC, Dong XW, Lai J, Feldman JL. Functional respiratory rhythm generating networks in neonatal mice lacking NMDAR1 gene. J Neurophysiol. 1997; 78:1414–1420. [PubMed: 9310432]

Funk GD, Smith JC, Feldman JL. Generation and transmission of respiratory oscillations in medullary slices: role of excitatory amino acids. J Neurophysiol. 1993; 70:1497–1515. [PubMed: 8283211]

Ge Q, Feldman JL. AMPA receptor activation and phosphatase inhibition affect neonatal rat respiratory rhythm generation. J Physiol. 1998; 509(Pt 1):255–266. [PubMed: 9547398]

Gibson HE, Edwards JG, Page RS, Van Hook MJ, Kauer JA. TRPV1 channels mediate long-term depression at synapses on hippocampal interneurons. Neuron. 2008; 57:746–759. [PubMed: 18341994]

Gosgnach S, Lanuza GM, Butt SJ, Saueressig H, Zhang Y, Velasquez T, Riethmacher D, Callaway EM, Kiehn O, Goulding M. V1 spinal neurons regulate the speed of vertebrate locomotor outputs. Nature. 2006; 440:215–219. [PubMed: 16525473]

Goulding M. Circuits controlling vertebrate locomotion: moving in a new direction. Nat Rev Neurosci. 2009; 10:507–518. [PubMed: 19543221]

Goulding M, Pfaff SL. Development of circuits that generate simple rhythmic behaviors in vertebrates. Curr Opin Neurobiol. 2005; 15:14–20. [PubMed: 15721739]

Gray PA, Janczewski WA, Mellen N, Mccrimmon DR, Feldman JL. Normal breathing requires preBötzinger complex neurokinin-1 receptor-expressing neurons. Nat Neurosci. 2001; 4:927–930. [PubMed: 11528424]

Gray PA, Rekling JC, Bocchiaro CM, Feldman JL. Modulation of respiratory frequency by peptidergic input to rhythmogenic neurons in the preBötzinger complex. Science. 1999; 286:1566–1568. [PubMed: 10567264]

Greer JJ, Smith JC, Feldman JL. Role of excitatory amino acids in the generation and transmission of respiratory drive in neonatal rat. J Physiol. 1991; 437:727–749. [PubMed: 1653855]

Grillner S. Biological pattern generation: the cellular and computational logic of networks in motion. Neuron. 2006; 52:751–766. [PubMed: 17145498]

Guyenet PG, Sevigny CP, Weston MC, Stornetta RL. Neurokinin-1 receptor-expressing cells of the ventral respiratory group are functionally heterogeneous and predominantly glutamatergic. J Neurosci. 2002; 22:3806–3816. [PubMed: 11978856]

Guyenet PG, Wang H. Pre-Bötzinger neurons with preinspiratory discharges "in vivo" express NK1 receptors in the rat. J Neurophysiol. 2001; 86:438–446. [PubMed: 11431523]

Hartelt N, Skorova E, Manzke T, Suhr M, Mironova L, Kugler S, Mironov SL. Imaging of respiratory network topology in living brainstem slices. Mol Cell Neurosci. 2008; 37:425–431. [PubMed: 18203620]

Hayes JA, Del Negro CA. Neurokinin Receptor-Expressing PreBötzinger Complex Neurons in Neonatal Mice Studied In Vitro. J Neurophysiol. 2007; 97:4215–4224. [PubMed: 17409172]

Hille, B. Ion Channels of Excitable Membranes, Third Edition. Sunderland, MA: Sinauer Associates; 2001.

Hinckley CA, Hartley R, Wu L, Todd A, Ziskind-Conhaim L. Locomotor-like rhythms in a genetically distinct cluster of interneurons in the mammalian spinal cord. J Neurophysiol. 2005; 93:1439–1449. [PubMed: 15496486]

Hinckley CA, Ziskind-Conhaim L. Electrical coupling between locomotor-related excitatory interneurons in the mammalian spinal cord. J Neurosci. 2006; 26:8477–8483. [PubMed: 16914672]

Hofmann T, Chubanov V, Gudermann T, Montell C. TRPM5 is a voltage-modulated and Ca(2+)-activated monovalent selective cation channel. Curr Biol. 2003; 13:1153–1158. [PubMed: 12842017]

Johnson SM, Smith JC, Funk GD, Feldman JL. Pacemaker behavior of respiratory neurons in medullary slices from neonatal rat. J Neurophysiol. 1994; 72:2598–2608. [PubMed: 7897477]

Johnson SM, Wiegel LM, Majewski DJ. Are pacemaker properties required for respiratory rhythm generation in adult turtle brain stems in vitro? Am J Physiol Regul Integr Comp Physiol. 2007; 293:R901–R910. [PubMed: 17522127]

Johnson SM, Wilkerson JE, Wenninger MR, Henderson DR, Mitchell GS. Role of synaptic inhibition in turtle respiratory rhythm generation. J Physiol. 2002; 544:253–265. [PubMed: 12356896]

Kettunen P, Kyriakatos A, Hallen K, El Manira A. Neuromodulation via conditional release of endocannabinoids in the spinal locomotor network. Neuron. 2005; 45:95–104. [PubMed: 15629705]

Kiehn O, Quinlan KA, Restrepo CE, Lundfald L, Borgius L, Talpalar AE, Endo T. Excitatory components of the mammalian locomotor CPG. Brain Res Rev. 2008; 57:56–63. [PubMed: 17988744]

Kogo M, Funk GD, Chandler SH. Rhythmical oral-motor activity recorded in an in vitro brainstem preparation. Somatosens Mot Res. 1996; 13:39–48. [PubMed: 8725647]

Koizumi H, Smerin SE, Yamanishi T, Moorjani BR, Zhang R, Smith JC. TASK Channels Contribute to the K+-Dominated Leak Current Regulating Respiratory Rhythm Generation In Vitro. J Neurosci. 2010; 30:4273–4284. [PubMed: 20335463]

Koizumi H, Smith JC. Persistent Na+ and K+-dominated leak currents contribute to respiratory rhythm generation in the pre-Bötzinger complex in vitro. J Neurosci. 2008; 28:1773–1785. [PubMed: 18272697]

Kolta A, Brocard F, Verdier D, Lund JP. A review of burst generation by trigeminal main sensory neurons. Arch Oral Biol. 2007; 52:325–328. [PubMed: 17178100]

Koshiya N, Smith JC. Neuronal pacemaker for breathing visualized in vitro. Nature. 1999; 400:360–363. [PubMed: 10432113]

Kosmidis EK, Pierrefiche O, Vibert JF. Respiratory-like rhythmic activity can be produced by an excitatory network of non-pacemaker neuron models. J Neurophysiol. 2004; 92:686–699. [PubMed: 15277592]

Kozlov A, Huss M, Lansner A, Kotaleski JH, Grillner S. Simple cellular and network control principles govern complex patterns of motor behavior. Proc Natl Acad Sci U S A. 2009; 106:20027–20032. [PubMed: 19901329]

Launay P, Fleig A, Perraud AL, Scharenberg AM, Penner R, Kinet JP. TRPM4 is a Ca2+-activated nonselective cation channel mediating cell membrane depolarization. Cell. 2002; 109:397–407. [PubMed: 12015988]

Liu D, Liman ER. Intracellular Ca2+ and the phospholipid PIP2 regulate the taste transduction ion channel TRPM5. Proc Natl Acad Sci U S A. 2003; 100:15160–15165. [PubMed: 14657398]

Marder E. Moving rhythms. Nature. 2001; 410:755. [PubMed: 11298422]

Marder E, Bucher D. Central pattern generators and the control of rhythmic movements. Curr Biol. 2001; 11:R986–R996. [PubMed: 11728329]

Marder E, Calabrese RL. Principles of rhythmic motor pattern generation. Physiol Rev. 1996; 76:687–717. [PubMed: 8757786]

Mckay LC, Janczewski WA, Feldman JL. Sleep-disordered breathing after targeted ablation of preBotzinger complex neurons. Nat Neurosci. 2005; 8:1142–1144. [PubMed: 16116455]

Mironov SL. Metabotropic glutamate receptors activate dendritic calcium waves and TRPM channels which drive rhythmic respiratory patterns in mice. J Physiol. 2008; 586:2277–2291. [PubMed: 18308826]

Morgado-Valle C, Baca SM, Feldman JL. Glycinergic Pacemaker Neurons in PreBötzinger Complex of Neonatal Mouse. J Neurosci. 2010; 30:3634–3639. [PubMed: 20219997]

Morgado-Valle C, Feldman JL. NMDA receptors in preBotzinger complex neurons can drive respiratory rhythm independent of AMPA receptors. J Physiol. 2007; 582:359–368. [PubMed: 17446224]

Onimaru H, Ballanyi K, Homma I. Contribution of Ca2+-dependent conductances to membrane potential fluctuations of medullary respiratory neurons of newborn rats in vitro. J Physiol. 2003; 552:727–741. [PubMed: 12937288]

Onimaru H, Ikeda K, Kawakami K. CO2-sensitive preinspiratory neurons of the parafacial respiratory group express Phox2b in the neonatal rat. J Neurosci. 2008; 28:12845–12850. [PubMed: 19036978]

Onimaru H, Ikeda K, Kawakami K. Phox2b, RTN/pFRG neurons and respiratory rhythmogenesis. Respir Physiol Neurobiol. 2009; 168:13–18. [PubMed: 19712902]

Paarmann I, Frermann D, Keller BU, Hollmann M. Expression of 15 glutamate receptor subunits and various splice variants in tissue slices and single neurons of brainstem nuclei and potential functional implications. J Neurochem. 2000; 74:1335–1345. [PubMed: 10737588]

Pace, RW. Applied Science. Williamsburg, Virginia: The College of William and Mary; 2007. Mechanisms underlying inspiratory burst generation in preBötzinger complex neurons of neonatal mice.

Pace RW, Del Negro CA. AMPA and metabotropic glutamate receptors cooperatively generate inspiratory-like depolarization in mouse respiratory neurons in vitro. Eur J Neurosci. 2008; 28:2434–2442. [PubMed: 19032588]

Pace RW, Mackay DD, Feldman JL, Del Negro CA. Inspiratory bursts in the preBötzinger Complex depend on a calcium-activated nonspecific cationic current linked to glutamate receptors. J Physiol. 2007a; 582:113–125. [PubMed: 17446214]

Pace RW, Mackay DD, Feldman JL, Del Negro CA. Role of persistent sodium current in mouse preBotzinger Complex neurons and respiratory rhythm generation. J Physiol. 2007b; 580:485–496. [PubMed: 17272351]

Pagliardini S, Adachi T, Ren J, Funk GD, Greer JJ. Fluorescent tagging of rhythmically active respiratory neurons within the pre-Botzinger complex of rat medullary slice preparations. J Neurosci. 2005; 25:2591–2596. [PubMed: 15758169]

Pena F, Parkis MA, Tryba AK, Ramirez JM. Differential Contribution of Pacemaker Properties to the Generation of Respiratory Rhythms during Normoxia and Hypoxia. Neuron. 2004; 43:105–117. [PubMed: 15233921]

Pena F, Ramirez JM. Substance P-mediated modulation of pacemaker properties in the mammalian respiratory network. J Neurosci. 2004; 24:7549–7556. [PubMed: 15329402]

Ptak K, Yamanishi T, Aungst J, Milescu LS, Zhang R, Richerson GB, Smith JC. Raphe neurons stimulate respiratory circuit activity by multiple mechanisms via endogenously released serotonin and substance P. J Neurosci. 2009; 29:3720–3737. [PubMed: 19321769]

Ptak K, Zummo GG, Alheid GF, Tkatch T, Surmeier DJ, Mccrimmon DR. Sodium currents in medullary neurons isolated from the pre-Bötzinger complex region. J Neurosci. 2005; 25:5159–5170. [PubMed: 15917456]

Ramsey IS, Delling M, Clapham DE. An introduction to trp channels. Annu Rev Physiol. 2006; 68:619–647. [PubMed: 16460286]

Rekling JC, Champagnat J, Denavit-Saubie M. Electroresponsive properties and membrane potential trajectories of three types of inspiratory neurons in the newborn mouse brain stem in vitro. J Neurophysiol. 1996a; 75:795–810. [PubMed: 8714653]

Rekling JC, Champagnat J, Denavit-Saubie M. Thyrotropin-releasing hormone (TRH) depolarizes a subset of inspiratory neurons in the newborn mouse brain stem in vitro. J Neurophysiol. 1996b; 75:811–819. [PubMed: 8714654]

Rekling JC, Feldman JL. PreBötzinger complex and pacemaker neurons: hypothesized site and kernel for respiratory rhythm generation. Annu Rev Physiol. 1998; 60:385–405. [PubMed: 9558470]

Rekling JC, Shao XM, Feldman JL. Electrical coupling and excitatory synaptic transmission between rhythmogenic respiratory neurons in the preBotzinger complex. J Neurosci. 2000; 20:RC113. [PubMed: 11090613]

Ren J, Greer JJ. Modulation of respiratory rhythmogenesis by chloride-mediated conductances during the perinatal period. J Neurosci. 2006; 26:3721–3730. [PubMed: 16597726]

Richter DW, Spyer KM. Studying rhythmogenesis of breathing: comparison of in vivo and in vitro models. Trends Neurosci. 2001; 24:464–472. [PubMed: 11476886]

Rinzel, J.; Ermentrout, B. Analysis of neural excitability and oscillations. In: Koch, C.; Segev, I., editors. Methods in neuronal modeling: from ions to networks. 2nd ed.. Cambridge, Mass: MIT Press; 1998.

Ritter B, Zhang W. Early postnatal maturation of GABAA-mediated inhibition in the brainstem respiratory rhythm-generating network of the mouse. Eur J Neurosci. 2000; 12:2975–2984. [PubMed: 10971638]

Rubin JE, Hayes JA, Mendenhall JL, Del Negro CA. Calcium-activated nonspecific cation current and synaptic depression promote network-dependent burst oscillations. Proc Natl Acad Sci U S A. 2009a; 106:2939–2944. [PubMed: 19196976]

Rubin JE, Shevtsova NA, Ermentrout GB, Smith JC, Rybak IA. Multiple rhythmic states in a model of the respiratory central pattern generator. J Neurophysiol. 2009b; 101:2146–2165. [PubMed: 19193773]

Rybak IA, Ptak K, Shevtsova NA, Mccrimmon DR. Sodium Currents in Neurons from the Rostroventrolateral Medulla of the Rat. J Neurophysiol. 2003; 90:1635–1642. [PubMed: 12761275]

Shao XM, Feldman JL. Respiratory rhythm generation and synaptic inhibition of expiratory neurons in pre-Botzinger complex: differential roles of glycinergic and GABAergic neural transmission. J Neurophysiol. 1997; 77:1853–1860. [PubMed: 9114241]

Smith JC, Abdala AP, Koizumi H, Rybak IA, Paton JF. Spatial and functional architecture of the mammalian brain stem respiratory network: a hierarchy of three oscillatory mechanisms. J Neurophysiol. 2007; 98:3370–3387. [PubMed: 17913982]

Smith JC, Ellenberger HH, Ballanyi K, Richter DW, Feldman JL. Pre-Bötzinger complex: a brainstem region that may generate respiratory rhythm in mammals. Science. 1991; 254:726–729. [PubMed: 1683005]

Smith, JC.; Funk, GD.; Johnson, SM.; Feldman, JL. Cellular and synaptic mechanisms generating respiratory rhythm: insights from in vitro and computational studies. In: Trouth, CO.; Millis, RM.; Kiwull-Schöne, HF.; Schläfke, ME., editors. Ventral brainstem mechanisms and control of respiration and blood pressure. New York, M: Dekker; 1995.

Stein, PSG.; Grillner, S.; Selverston, AI.; Stuart, DG. Neurons, networks, and motor behavior. Cambridge: MIT Press; 1997.

Stornetta RL, Rosin DL, Wang H, Sevigny CP, Weston MC, Guyenet PG. A group of glutamatergic interneurons expressing high levels of both neurokinin-1 receptors and somatostatin identifies the region of the pre-Bötzinger complex. J Comp Neurol. 2003; 455:499–512. [PubMed: 12508323]

Stuart, G.; Spruston, N.; Häusser, M. Dendrites. Oxford ; New York: Oxford University Press; 2007.

Suzue T. Respiratory rhythm generation in the in vitro brain stem-spinal cord preparation of the neonatal rat. J Physiol. 1984; 354:173–183. [PubMed: 6148410]

Tan W, Janczewski WA, Yang P, Shao XM, Callaway EM, Feldman JL. Silencing preBotzinger Complex somatostatin-expressing neurons induces persistent apnea in awake rat. Nat Neurosci. 2008; 11:538–540. [PubMed: 18391943]

Tanaka S, Kogo M, Chandler SH, Matsuya T. Localization of oral-motor rhythmogenic circuits in the isolated rat brainstem preparation. Brain Res. 1999; 821:190–199. [PubMed: 10064803]

Teulon, J. Ca2+-activated nonselective cation channels. In: Endo, M.; Kurachi, Y.; Mishina, M., editors. Pharmacology of ionic channel function: activators and inhibitors. Berlin: Springer-Verlag; 2000.

Thoby-Brisson M, Ramirez JM. Identification of two types of inspiratory pacemaker neurons in the isolated respiratory neural network of mice. J Neurophysiol. 2001; 86:104–112. [PubMed: 11431492]

Urbani A, Belluzzi O. Riluzole inhibits the persistent sodium current in mammalian CNS neurons. Eur J Neurosci. 2000; 12:3567–3574. [PubMed: 11029626]

Wang H, Stornetta RL, Rosin DL, Guyenet PG. Neurokinin-1 receptor-immunoreactive neurons of the ventral respiratory group in the rat. J Comp Neurol. 2001; 434:128–146. [PubMed: 11331521]

Wenninger JM, Pan LG, Klum L, Leekley T, Bastastic J, Hodges MR, Feroah T, Davis S, Forster HV. Small reduction of neurokinin-1 receptor-expressing neurons in the pre-Bötzinger complex area

induces abnormal breathing periods in awake goats. J Appl Physiol. 2004a; 97:1620–1628. [PubMed: 15247160]

Wenninger JM, Pan LG, Klum L, Leekley T, Bastastic J, Hodges MR, Feroah TR, Davis S, Forster HV. Large lesions in the pre-Bötzinger complex area eliminate eupneic respiratory rhythm in awake goats. J Appl Physiol. 2004b; 97:1629–1636. [PubMed: 15247161]

Wilson JM, Blagovechtchenski E, Brownstone RM. Genetically defined inhibitory neurons in the mouse spinal cord dorsal horn: a possible source of rhythmic inhibition of motoneurons during fictive locomotion. J Neurosci. 2010; 30:1137–1148. [PubMed: 20089922]

Wilson JM, Cowan AI, Brownstone RM. Heterogeneous electrotonic coupling and synchronization of rhythmic bursting activity in mouse Hb9 interneurons. J Neurophysiol. 2007; 98:2370–2381. [PubMed: 17715199]

Wilson JM, Hartley R, Maxwell DJ, Todd AJ, Lieberam I, Kaltschmidt JA, Yoshida Y, Jessell TM, Brownstone RM. Conditional rhythmicity of ventral spinal interneurons defined by expression of the Hb9 homeodomain protein. J Neurosci. 2005; 25:5710–5719. [PubMed: 15958737]

Zavala-Tecuapetla C, Aguileta MA, Lopez-Guerrero JJ, Gonzalez-Marin MC, Pena F. Calcium-activated potassium currents differentially modulate respiratory rhythm generation. Eur J Neurosci. 2008; 27:2871–2884. [PubMed: 18445052]

Zhang Z, Okawa H, Wang Y, Liman ER. Phosphatidylinositol 4,5-bisphosphate rescues TRPM4 channels from desensitization. J Biol Chem. 2005; 280:39185–39192. [PubMed: 16186107]

Zhong G, Droho S, Crone SA, Dietz S, Kwan AC, Webb WW, Sharma K, Harris-Warrick RM. Electrophysiological characterization of V2a interneurons and their locomotor-related activity in the neonatal mouse spinal cord. J Neurosci. 2010; 30:170–182. [PubMed: 20053899]

LIST OF ABBREVIATIONS

AMPA	α-amino-3-hydroxy-5-methyl-4-isoxazole propionic acid
$I_{K\text{-}ATP}$	ATP-dependent K^+ current
aug-E	augmenting-expiratory
I_{CAN}	Ca^{2+}-activated nonspecific cationic current
CPG	central pattern generator
FFA	flufenamic acid
GABA	gamma-aminobutyric acid
XII	hypoglossal
IP_3	hypoglossal (XII) inositol 1,4,5-trisphosphate
$I_{K\text{-}Leak}$	leakage K^+ current
mGluRs	metabotropic glutamate receptors
$I_{K\text{-}Na}$	Na^+-dependent K^+ current
I_{pump}	Na^+/K^+ ATPase pump
NK1R	N-(2,6-Dimethylphenylcarbamoylmethyl)triethylammonium bromide (QX-314) neurokinin-1 receptor
IEM-1460	N,N,N,-Trimethyl-5-[(tricyclo[3.3.1.13,7]dec-1-ylmethyl) amino]-1-pentanaminiumbromide hydrobromide
NMDA	*N*-methyl-D-aspartate
I_{NaP}	persistent Na^+ current
PLC	phospholipase C

post-I	post-inspiratory
RIL	preBötzinger Complex; preBötC riluzole
SP	substance P
TTX	tetrodotoxin
TRP	*transient receptor potential*
GYKI 53655	1-(4-aminophenyl)-4-methyl-7,8-methylenedioxy-5H-2,3-benzodiazepine
BAPTA	1,2-bis(o-aminophenoxy)ethane-N,N,N',N'-tetraacetic acid

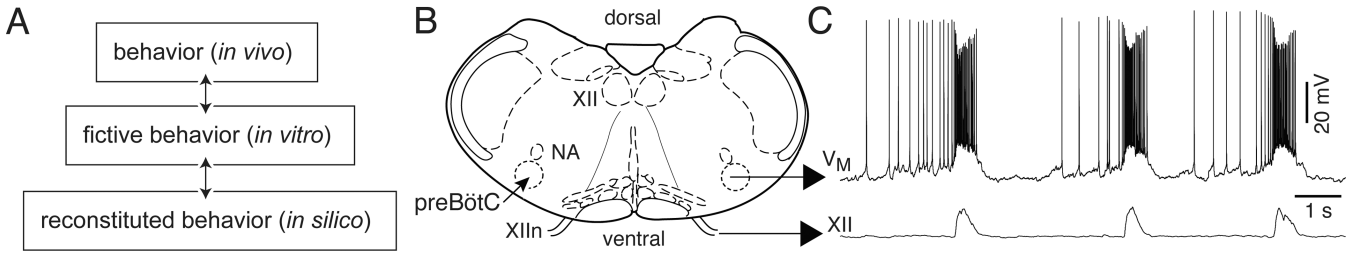

Figure 1.

The neural control of breathing studied at multiple levels. **A**) Hierarchy of model systems from breathing studied *in vivo* to reduced preparations *in vitro*, which includes *en bloc* brain stem-spinal cords and slices, and finally to *in silico* mathematical models. **B**) A cartoon of the slice preparation from neonatal rodents *in vitro*. **C**) Whole-cell patch-clamp recording of a preBötC neuron with XII respiratory motor output in a slice preparation.

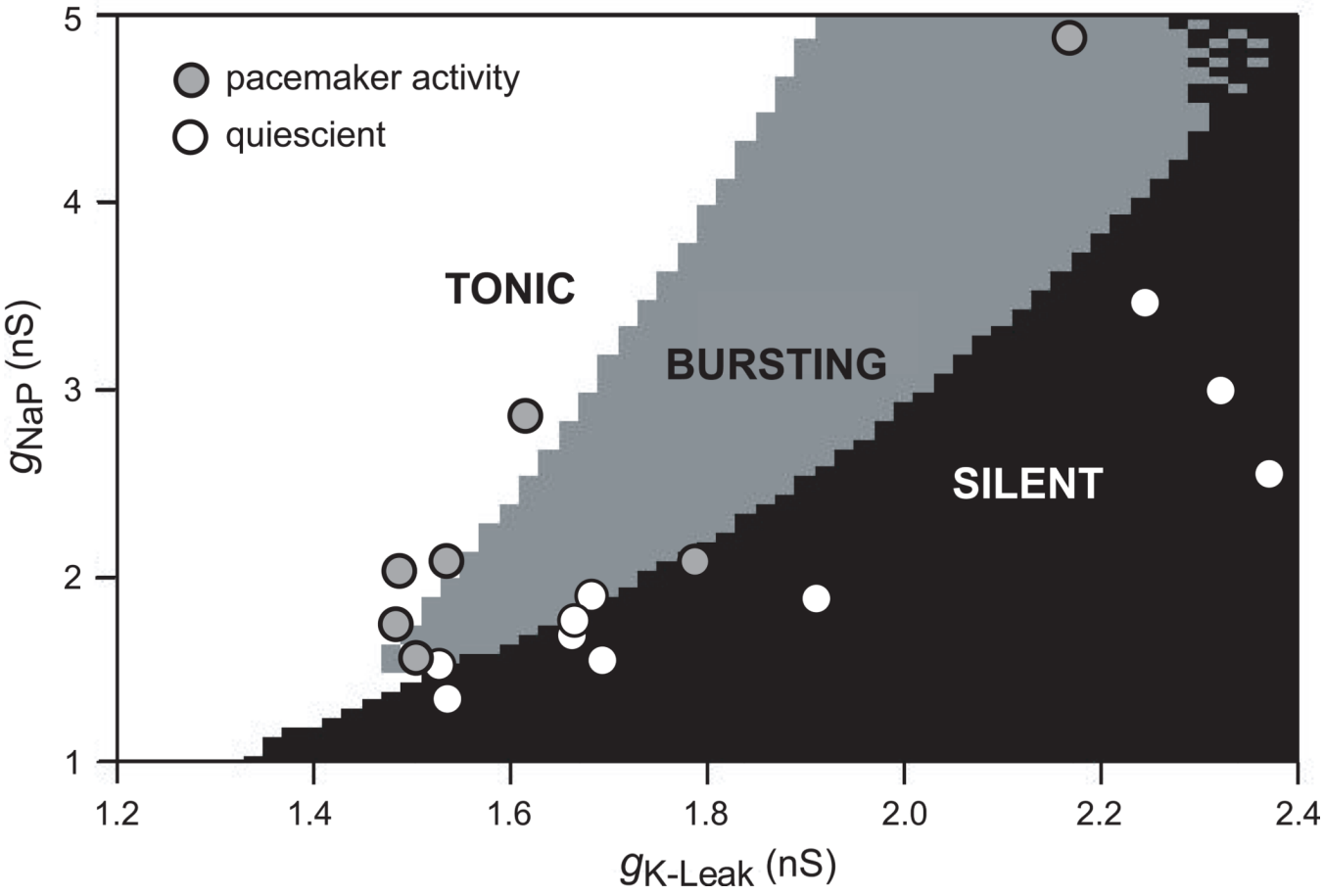

Figure 2.

Pacemaker properties in preBötC neurons are a natural byproduct of heterogeneity. The distribution of g_{NaP} vs. $g_{K\text{-}Leak}$ in the model proposed by Butera and colleagues in 1999 demonstrates that pacemaker properties are expected in 5–25% of constituent neurons. The white area of the plot denotes tonically active neurons; the gray area reflects bursting pacemaker activity; and finally the black area indicates a quiescent state. Superimposed experimental data points were obtained from whole-cell recordings of preBötC neurons in neonatal rats. The two-tuple (g_{NaP}, $g_{K\text{-}Leak}$) was added to the existing g_{NaP} vs. $g_{K\text{-}Leak}$ plot from the model, and the points were color-coded based on whether the recorded neurons showed pacemaker activity after synaptic isolation. The data matched the theoretical distribution, indicating that the ratio of $g_{NaP}/g_{K\text{-}Leak}$ governs whether intrinsic bursting is possible in any given neuron. This suggests that pacemaker properties are not specialized, but rather a natural byproduct of heterogeneity in a network of cells that all express g_{NaP} and $g_{K\text{-}Leak}$.

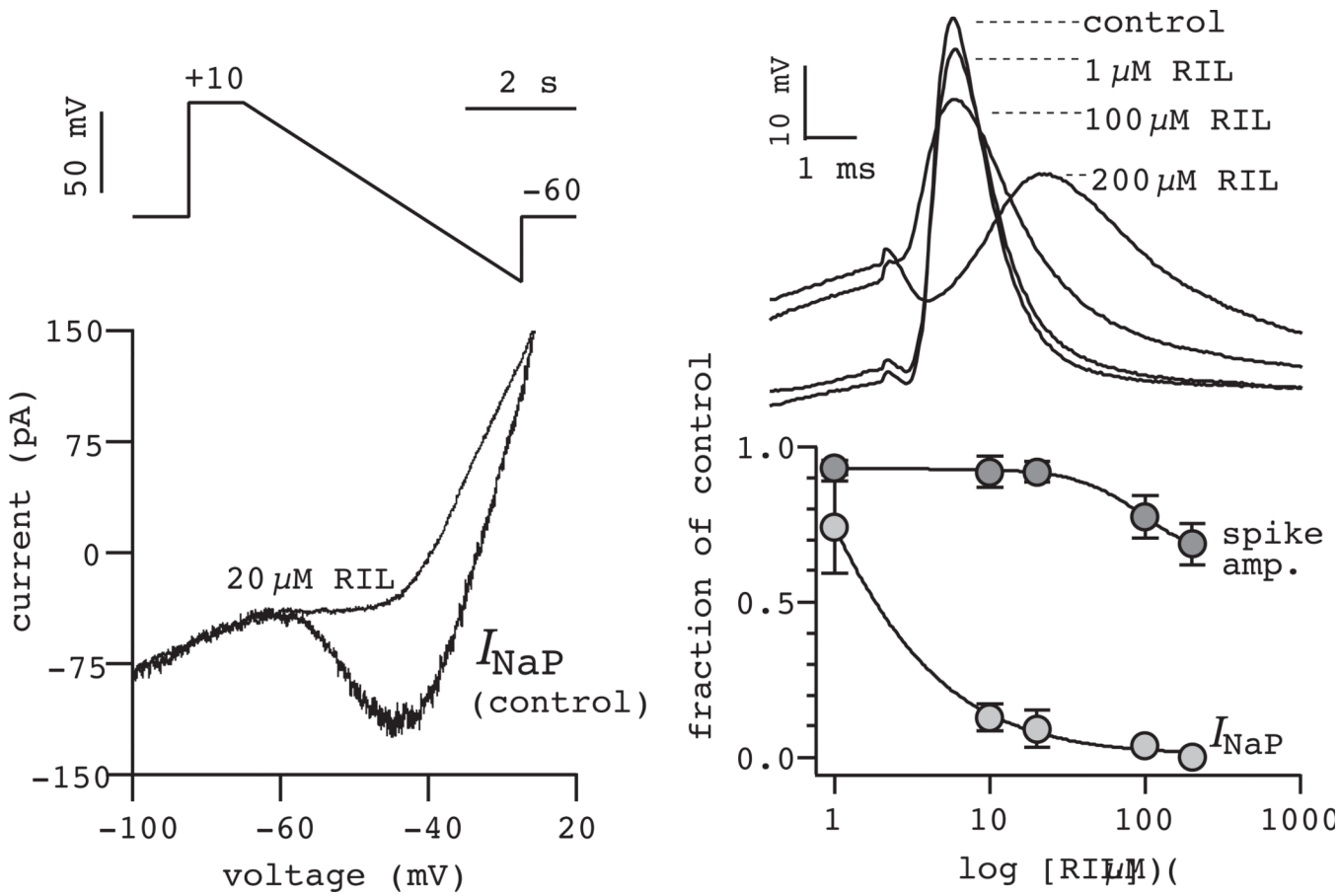

Figure 3.

Riluzole blocks I_{NaP}. Steady-state IV curves in control and 20 μM RIL (lower left) obtained from slow voltage-ramp commands (upper left). The effects of 1–200 μM RIL on action potentials evoked by 3-ms step current commands (upper right). A dose response curve shows the effects of RIL on I_{NaP} and on spike amplitude (lower right). Data modified and reprinted with permission from Del Negro, Morgado-Valle, and Feldman (2002) Neuron, 34, 821–30.

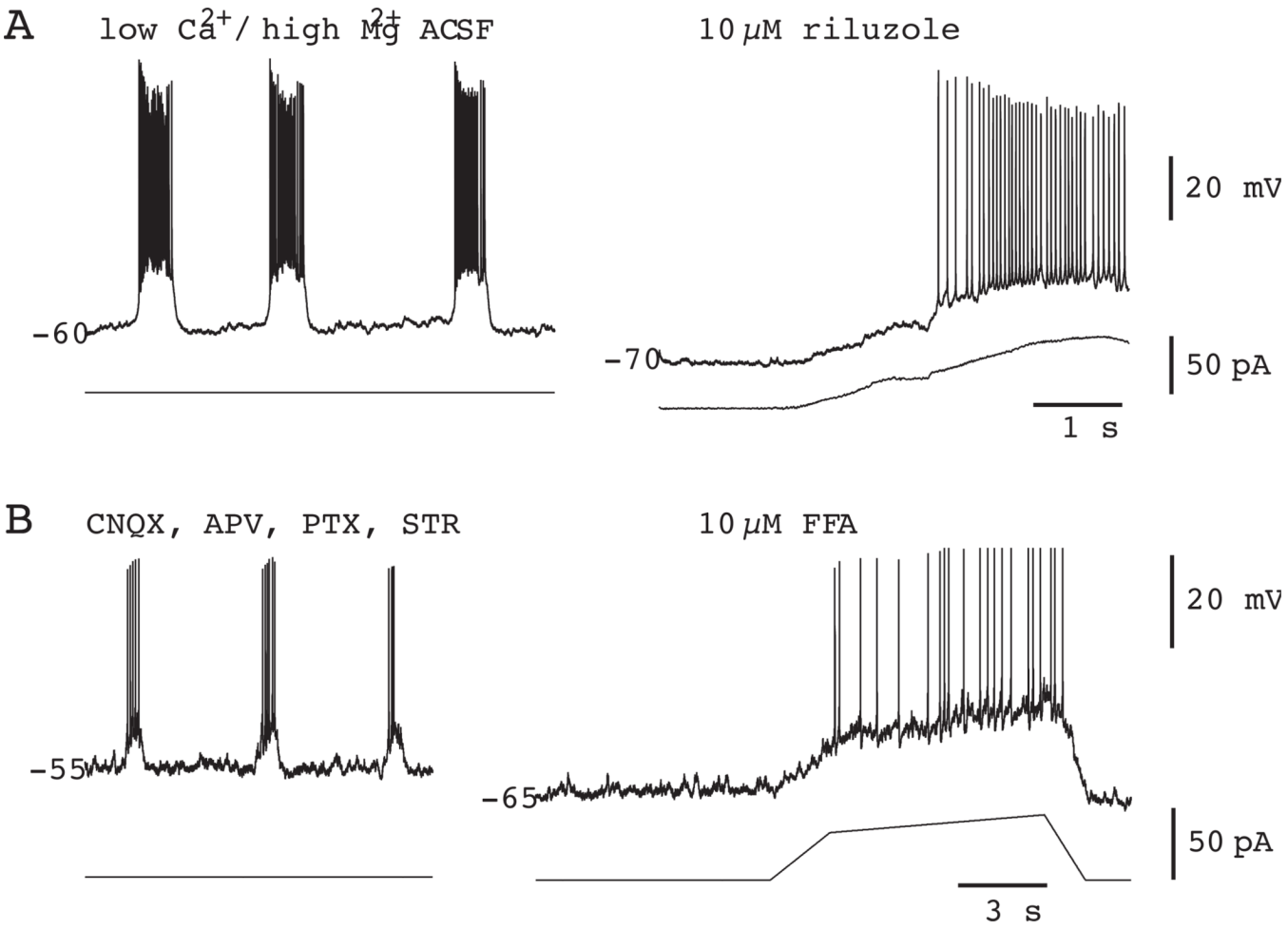

Figure 4.

Pharmacology of intrinsic bursting in preBötC neurons. **A**) 10 μM RIL blocks I^{NaP}-dependent bursting in a representative preBötC neuron synaptically isolated using low Ca^{2+} / high Mg^{2+} artificial cerebrospinal fluid (ACSF). **B**) 10 μM FFA blocks I_{CAN}-dependent bursting in a representative preBötC neuron. 6-cyano-7-nitroquinoxaline-2,3-dione (CNQX), 2-amino-5-phosphonopentanoic acid (APV), picrotoxin (PTX), and strychnine hydrochloride (STR) are excitatory synaptic receptor antagonists used to synaptically isolate the neuron in B. In both A and B the baseline membrane potential was ramped from −70 to −40 to test (unsuccessfully) for the presence of voltage-dependent bursting activity. Some plotted data were modified with permission from Del Negro *et al.* (2005) J Neurosci, 25, 446–53.

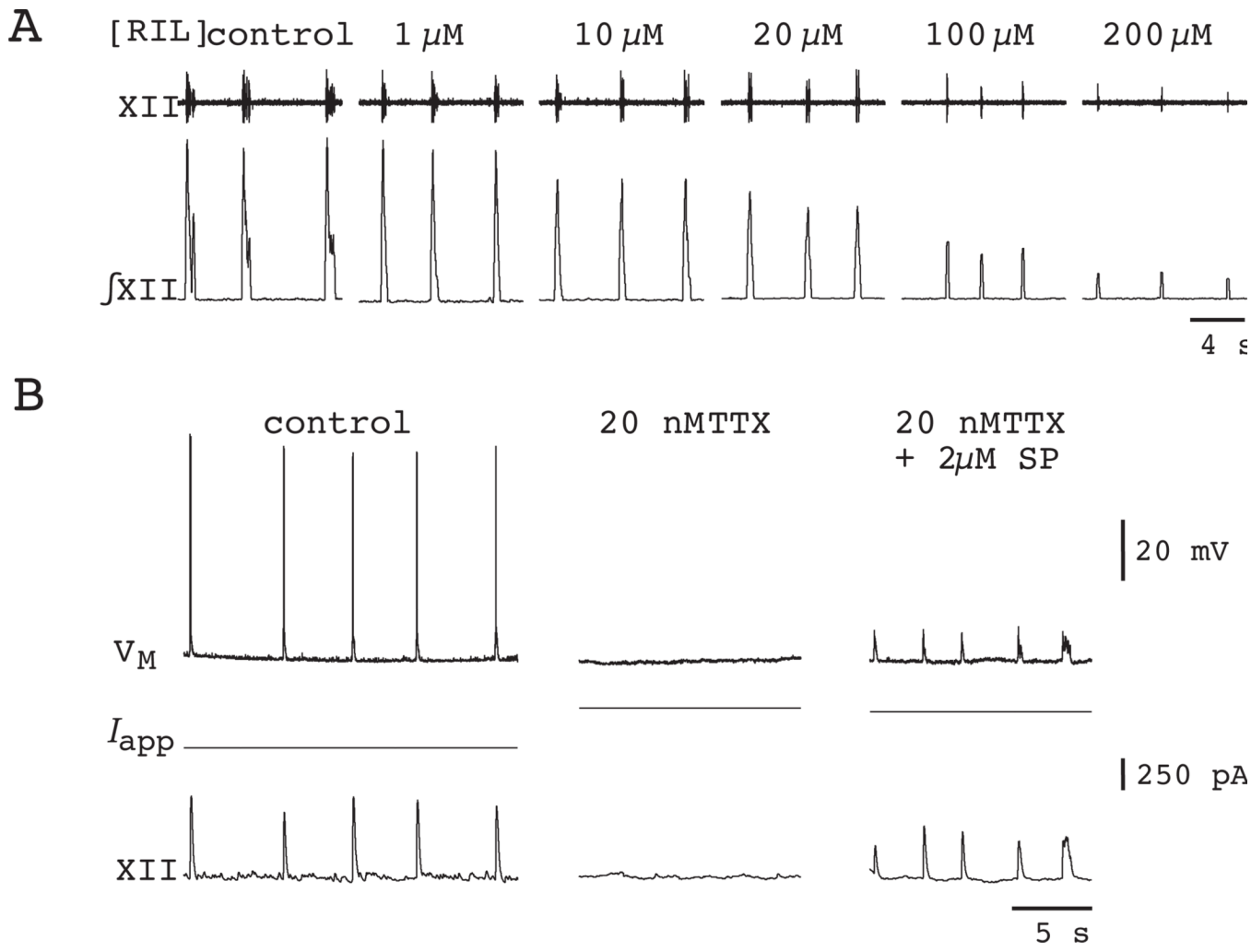

Figure 5.

The effects of RIL on respiratory motor rhythm and inspiratory preBötC neurons recorded *in vitro*. A) Motor activity recorded from the hypoglossal nerve (XII) in a cumulative dose-response experiment. RIL concentration is displayed above each trace. Raw and integrated traces (XII) are shown. B) Substance P (SP) at 2 μM restores respiratory rhythm in a mouse slice exposed to 20 nM TTX. This inspiratory neuron hyperpolarized by 7 mV in TTX, therefore +250 pA was applied (I_{app}) to restore baseline V_M to −60 mV. After the rhythm stopped, 2 μM SP revived it. The amplitude of the cellular drive potentials and XII amplitude recovered in SP, but spike discharge did not occur with baseline VM at −60 mV. Data have been modified with permission from Del Negro *et al.* (2002) Neuron, 34, 821–30; and Del Negro *et al.* (2005) J Neurosci, 25, 446–53.

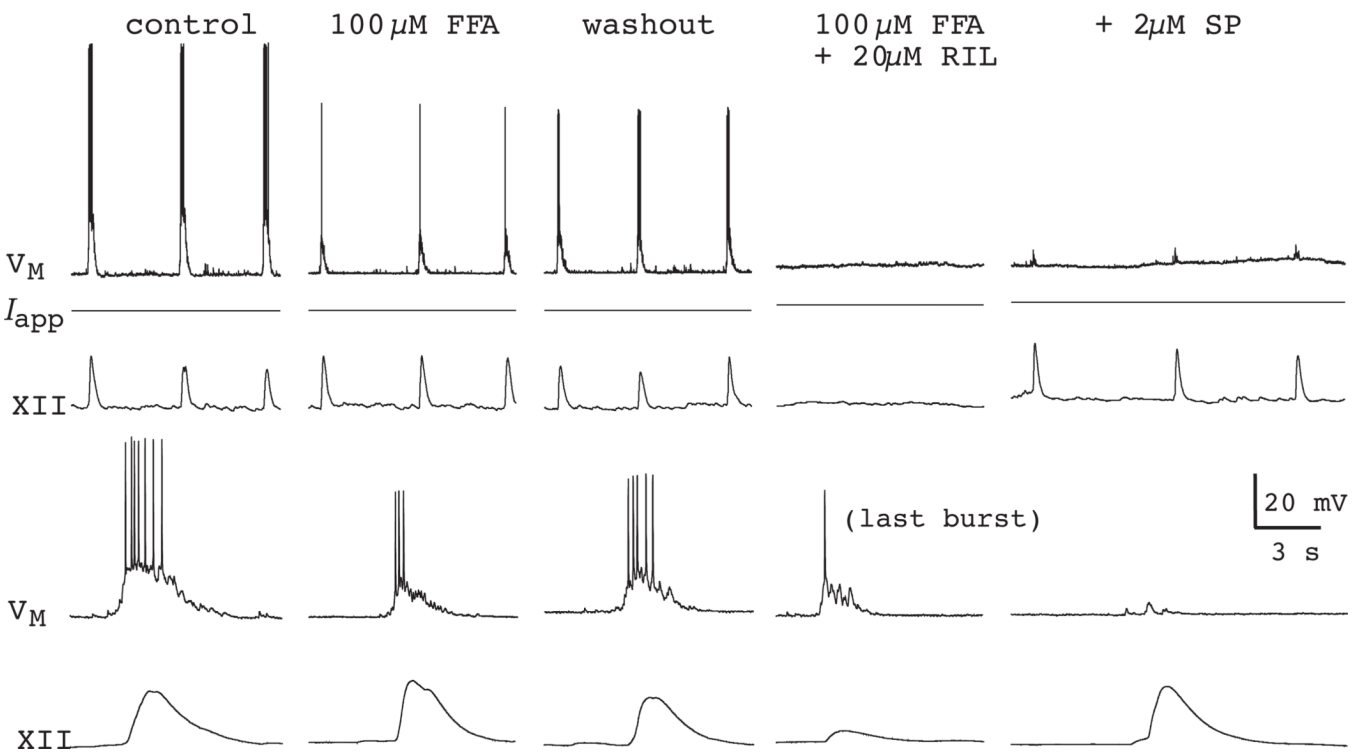

Figure 6.

Respiratory rhythm in the presence of 100 μM FFA and 20 μM RIL. Continuous segments of the experiment showing control, FFA, recovery, and then FFA + RIL co-application, and finally FFA + RIL + 2 μM SP conditions in a mouse slice. SP rescued the rhythm after its cessation due to FFA + RIL. Examples of inspiratory bursts and XII output are shown with greater time resolution (lower panels). Data have been modified with permission from Del Negro *et al.* (2005) J Neurosci, 25, 446–53.

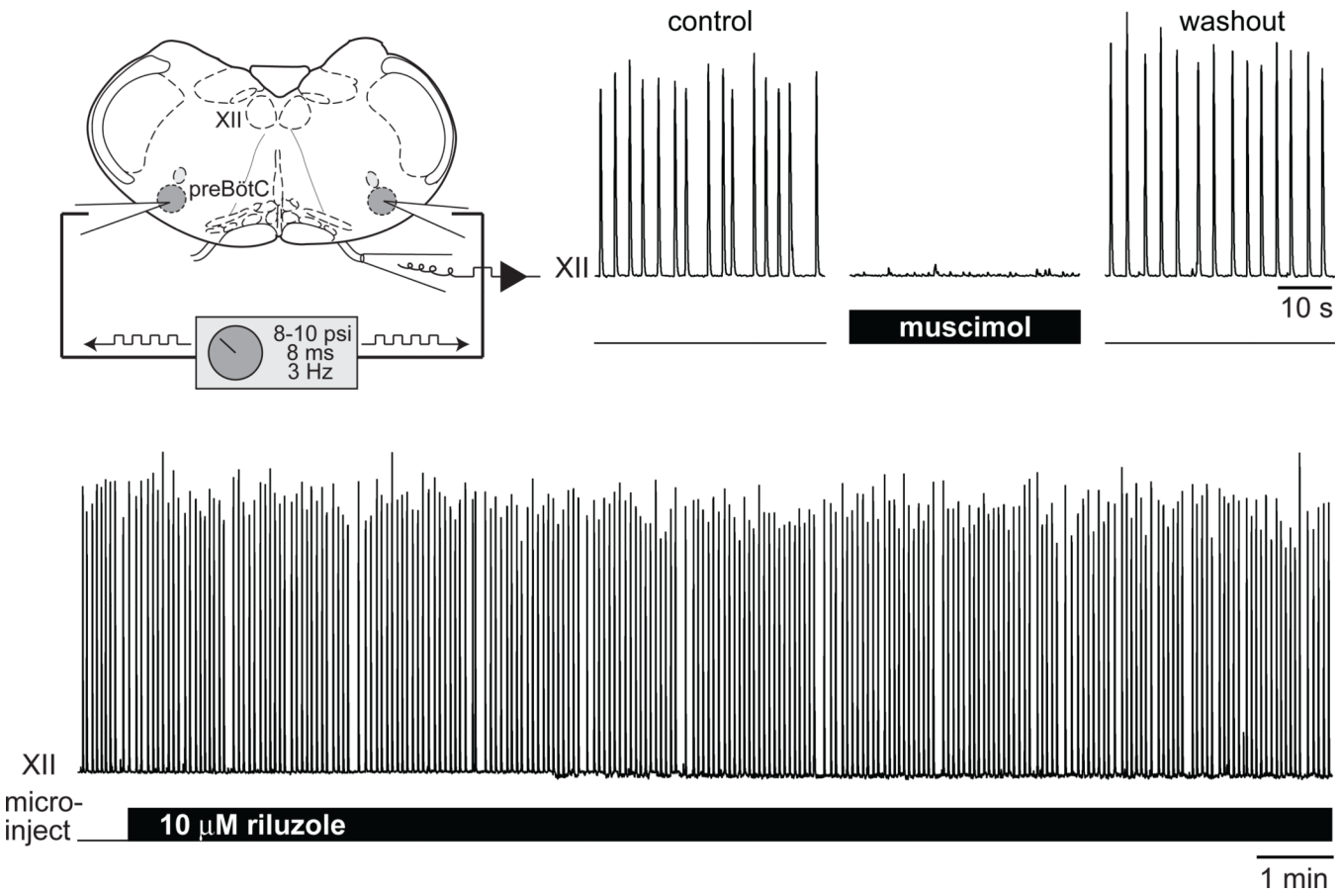

Figure 7.

Microinjection of RIL into the preBötC does not perturb respiratory rhythm. Bilateral microinjection of muscimol is a positive control to ensure the correct placement of the pipettes in the preBötC. After recovery from muscimol, 10 μM RIL microinjection has no effect on XII motor amplitude or frequency for >30 min. Original data are displayed in the figure, but similar experiments, and a more complete set of pharmacological conditions, can be found in: Pace *et al.* (2007) J Physiol, 580, 485–96.

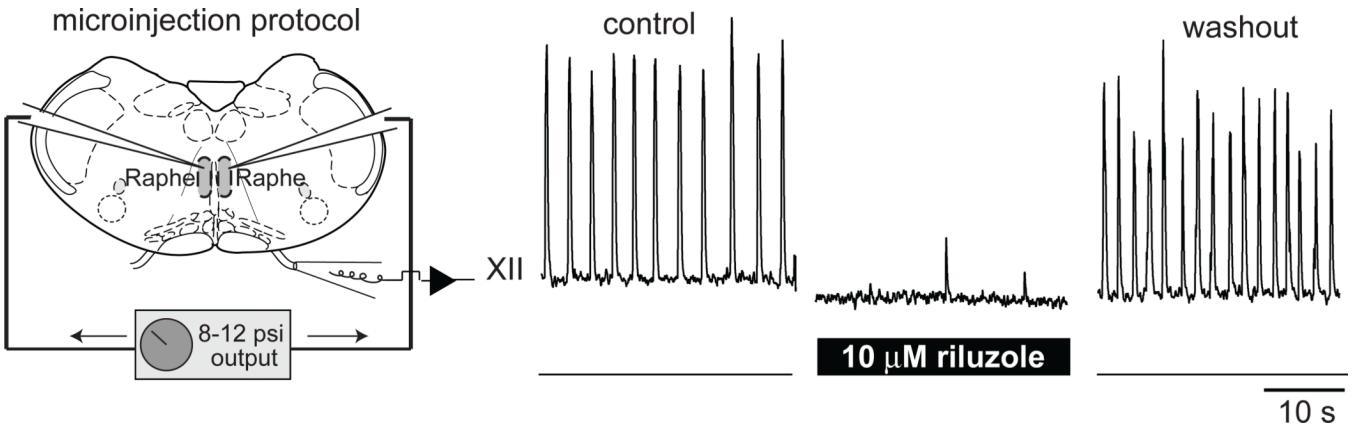

Figure 8.
Microinjection of RIL into the midline Raphé region stops respiratory rhythm *in vitro*. Plotted data have been modified with author permission from Pace *et al.* (2007) J Physiol, 580, 485–96.

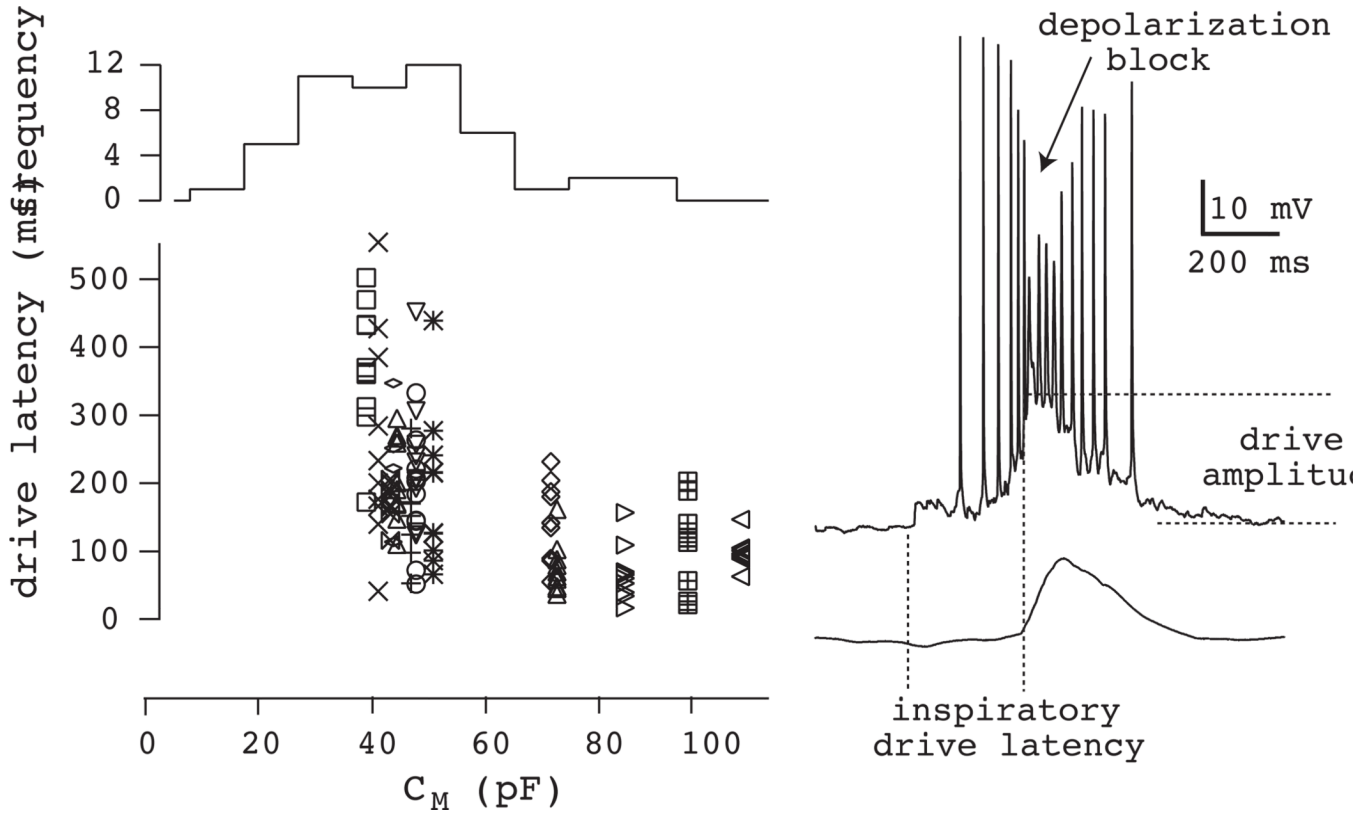

Figure 9.

Intrinsic properties of $NK1R^+$ preBötC neurons. Inspiratory drive latency is plotted versus whole-cell capacitance (C_M) in the lower graph. Histogram (top) shows the frequency of $NK1R^+$ neurons with C_M separated into 10-pF bins. Note that small (i.e., low C_M) $NK1R^+$ neurons predominate in the preBötC. A fast sweep of a typical inspiratory burst is shown at right with a diagram of characteristic measures (inspiratory drive latency and drive amplitude). Depolarization block of intraburst spike frequency is also indicated, which may have functional significance (see Fig. 16). Some data have been modified with permission from Hayes and Del Negro (2007) J Neurophysiol, 97, 4215–24.

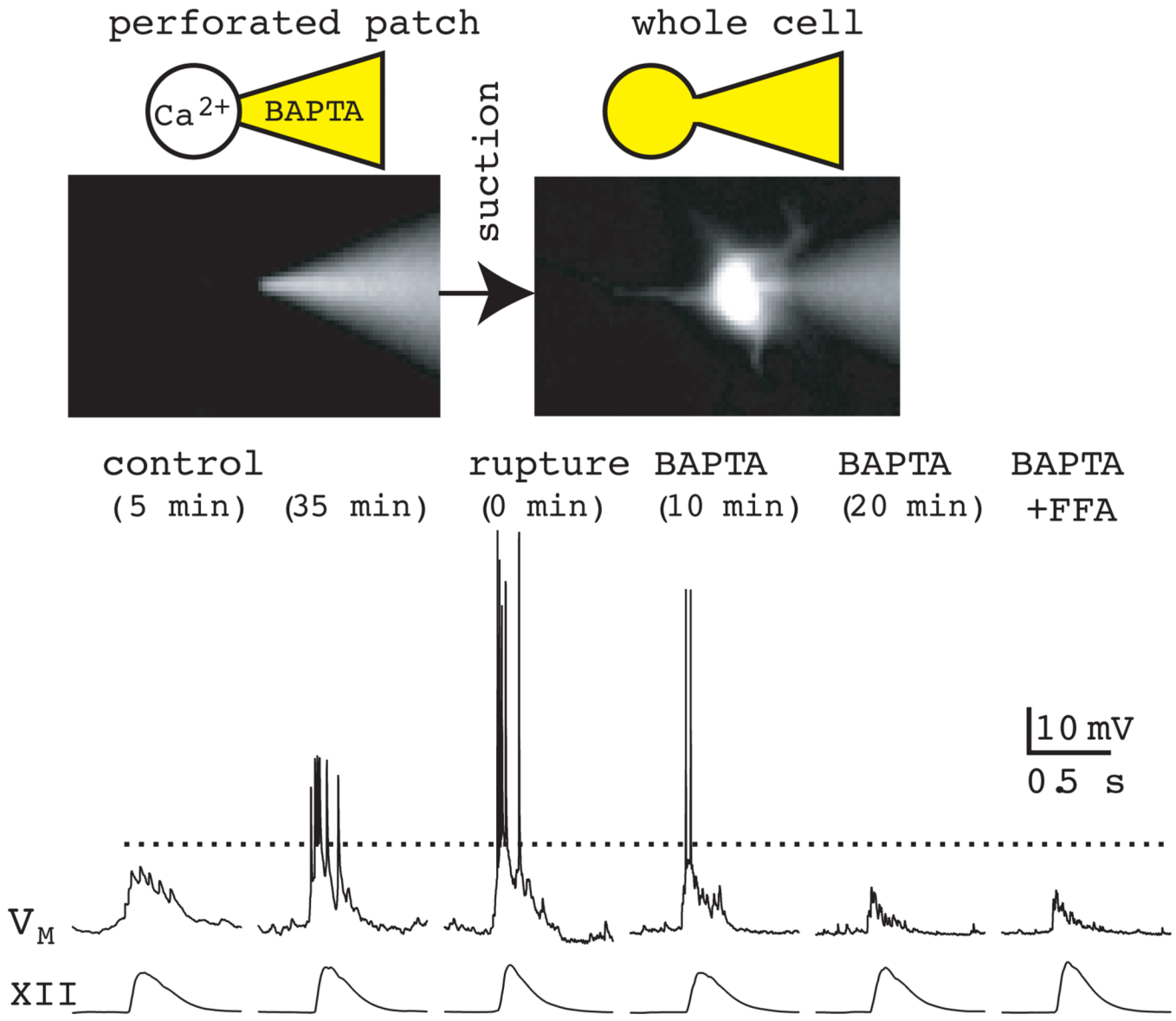

Figure 10.

Role of I_{CAN} in generating inspiratory bursts: chelation of intracellular Ca^{2+} by BAPTA attenuates inspiratory drive potentials. Patch-electrode filling solution contained 30 mM K_4-BAPTA as well as Lucifer yellow. The perforated-patch configuration (left cartoon and photo) is confirmed by the failure of the Lucifer yellow in the patch-pipette solution to dialyze the neuron. The whole-cell configuration (right cartoon and photo) allows Lucifer yellow to fill the neuron. Control conditions in perforated patch are shown at 5 and 35 min. BAPTA is introduced into the cytosol via patch rupture and causes a progressive attenuation of the inspiratory burst. Subsequent bath-application of 100 μM FFA has no additional attenuating effects even after 15 min of exposure to the drug. Baseline membrane potential was −60 mV throughout the experiment. Dotted line is drawn to facilitate comparison of the size of the inspiratory drive potential at different time points during the experiment. Data have been modified with author permission from Pace *et al.* (2007) J Physiol, 582, 113–25.

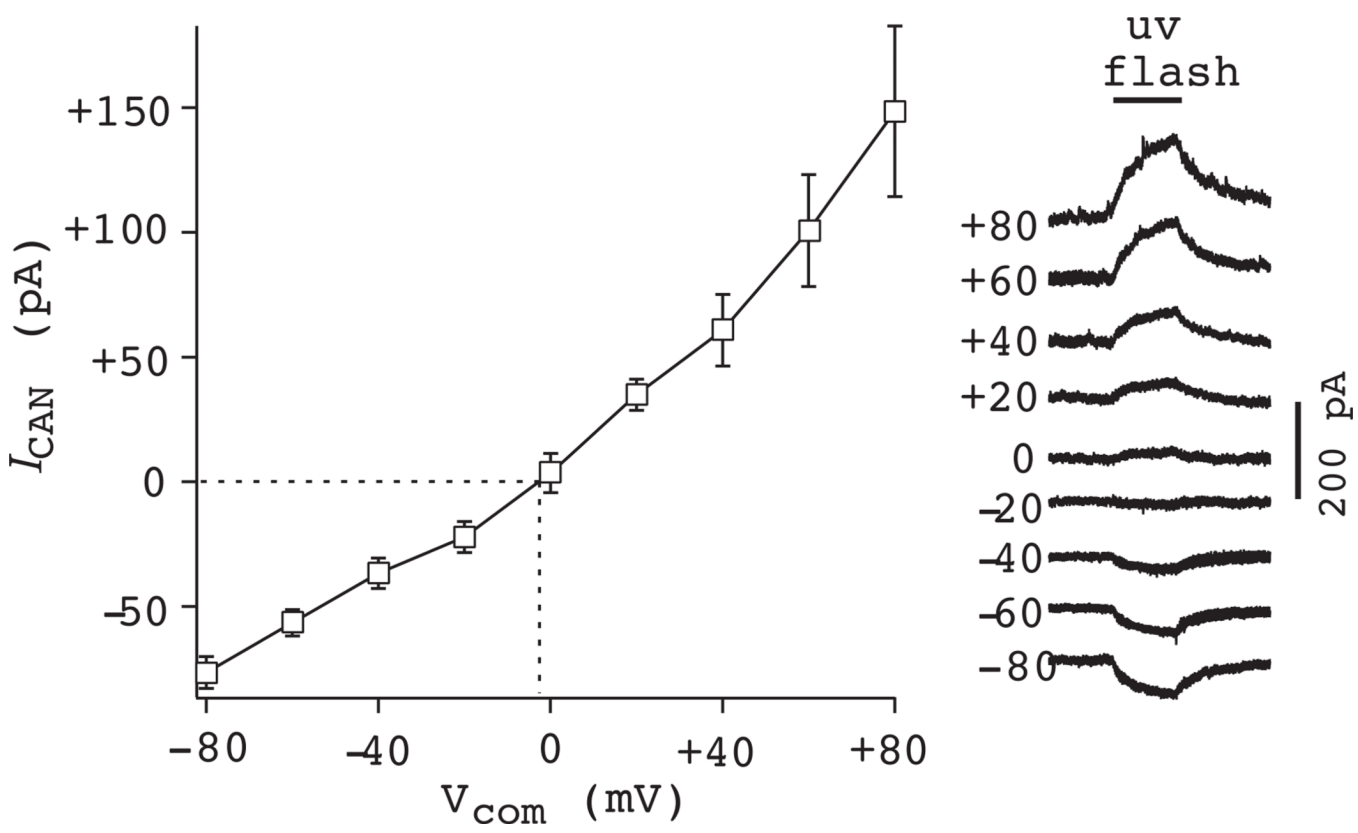

Figure 11.

Role of I_{CAN} in preBötC neurons: Ca^{2+} uncaging by ultraviolet illumination of the photolyzable chelator DM-Nitrophen. I_{CAN} was measured at a range of membrane potentials in voltage clamp. I_{CAN} reversed at ~0 mV, consistent with a mixed monovalent cation current. Similar data were obtained in current clamp (not shown).

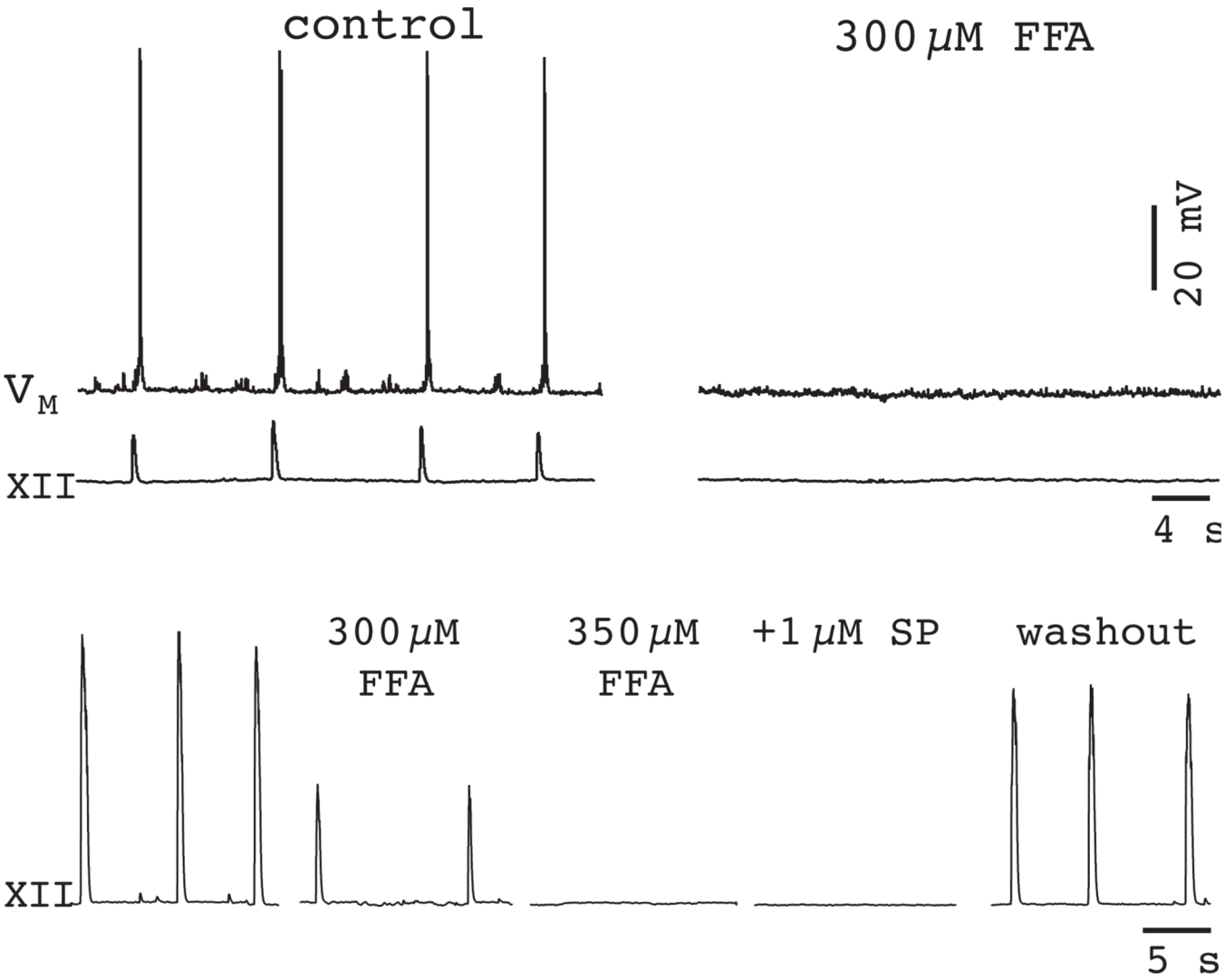

Figure 12.

A high dose of FFA (300 μM) blocks inspiratory activity in 70% of slices (top traces). 350-μM FFA blocks the respiratory rhythm in the other 30% (bottom traces). 1-μM substance P (SP) does not restart the rhythm in 350 μM FFA, but rhythmic activity does recover after > 1 h of washout. Baseline membrane potential was −60 mV for traces in the top. Data have been modified with author permission from Pace *et al.* (2007) J Physiol, 582, 113–25.

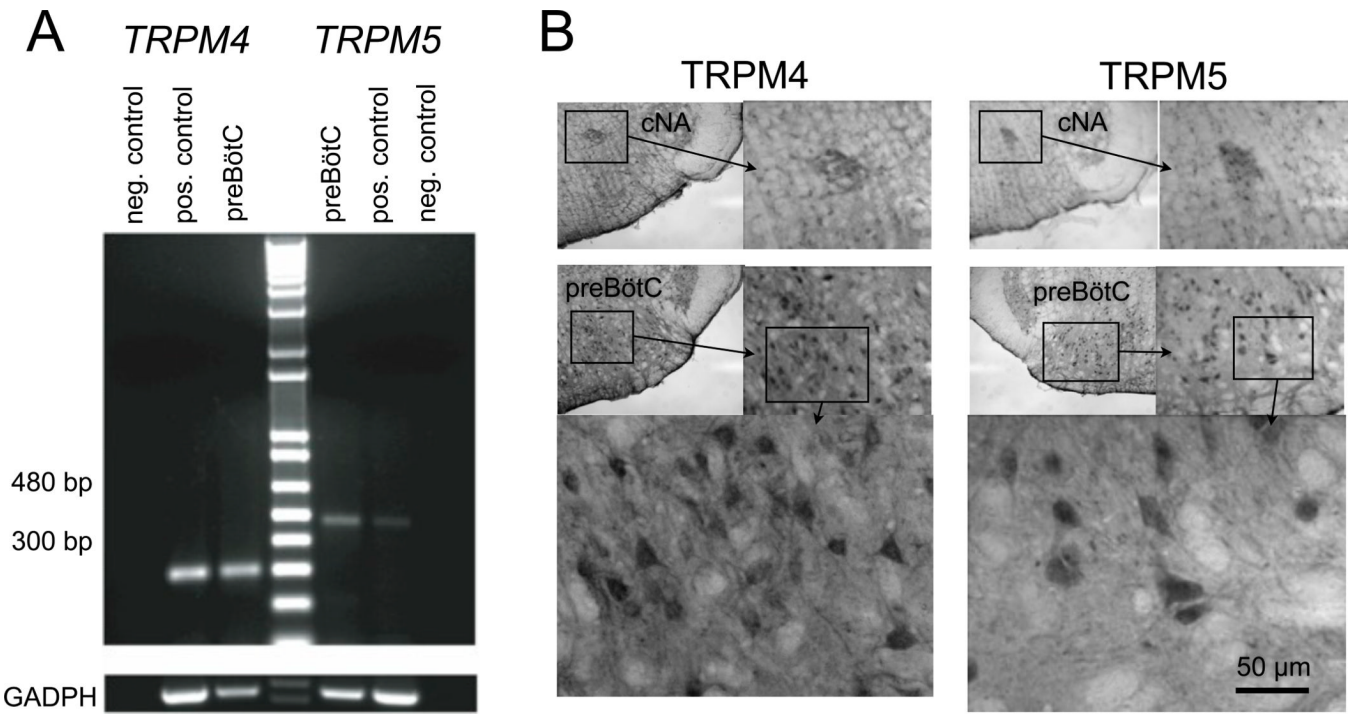

Figure 13.

Evidence for TRPM4 and TRPM5 channels in the preBötC. **A**) The mRNA coding for TRPM4 and TRPM5 is expressed in the preBötC region. Total RNA was extracted from preBötC and positive control tissues, and then reverse transcribed. Amplified products of the expected sizes were obtained for TRPM4 (301 bp), TRPM5 (483 bp) and GADPH (452 bp). Negative control reactions were performed without reverse transcriptase and amplified nothing. **B**) Immunohistochemistry from adult rats. Top panels (positive controls) show TRPM4 and TRPM5 in the compact nucleus ambiguous (cNA) taken from the ventral medulla immediately rostral to preBötC. Lower panels show TRPM4 and TRPM5 labeling in the preBötC at increasing magnification. Data in A were re-plotted with author permission from Crowder *et al.* (2007) J Physiol, 582, 1047–58.

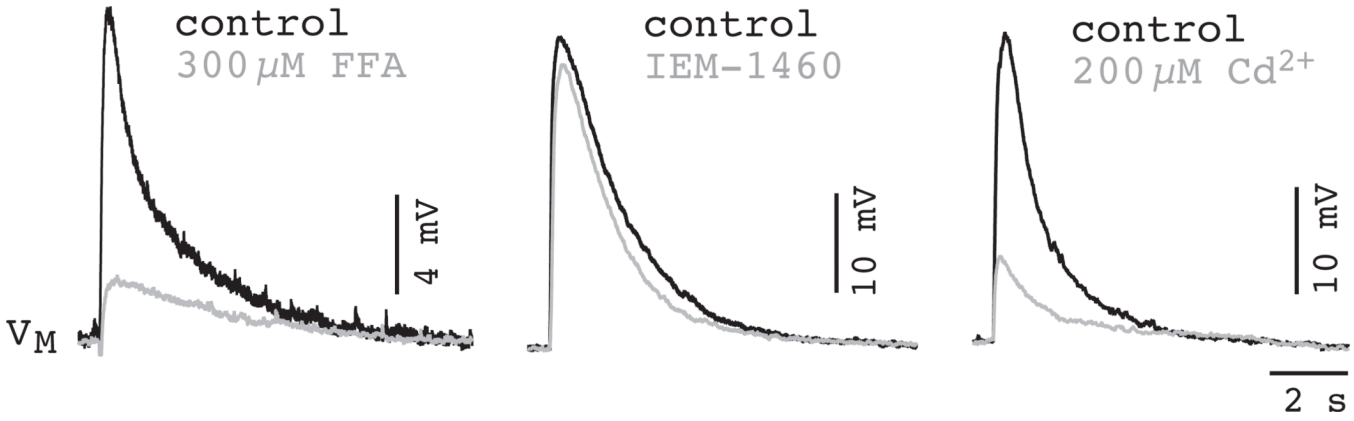

Figure 14.

AMPA receptor-mediated depolarization triggers I_{CAN} activation via Ca^{2+} channels. **A**) FFA (300 μM) significantly attenuates the AMPA receptor depolarization. **B**) N,N,N,-Trimethyl-5-[(tricyclo[3.3.1.13,7]dec-1-ylmethyl)amino]-1-pentanaminiumbromide hydrobromide (IEM-1460) (100 μM), a Ca2+- permeable AMPA receptor antagonist, does not perturb the AMPA receptor depolarization. **C**) Cd^{2+} attenuates the AMPA receptor depolarization (200 μM). Plotted data have been modified with author permission from Pace *et al.* (2008) Eur J Neurosci, 28, 2434–42.

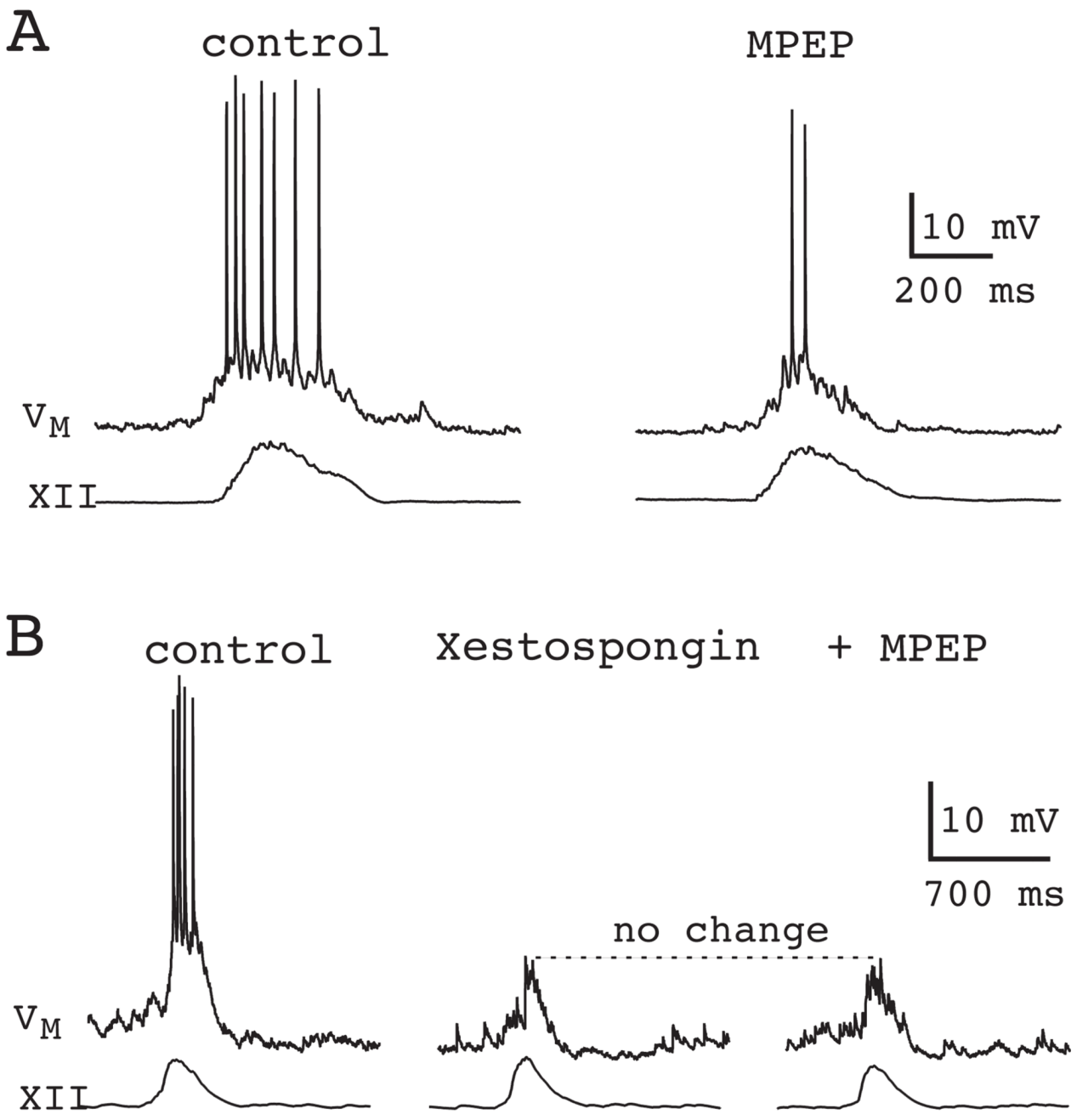

Figure 15.

Role of mGluR5 in inspiratory burst generation. **A**) Bath application of the selective mGluR5 antagonist MPEP (10 μM) attenuates inspiratory bursts in the context of ongoing network rhythm. **B**) Downstream of mGluR5, IP_3 receptors cause intracellular Ca^{2+} release and lead to I_{CAN} activation. Perforated-patch recordings serve as control. The IP_3 receptor antagonist xestospongin (1 μM), applied intracellularly by patch rupture, reduces inspiratory bursts. Subsequent application of MPEP causes no further change in the drive potential. Data have been modified with author permission from Pace *et al.* (2007) J Physiol, 582, 113–25.

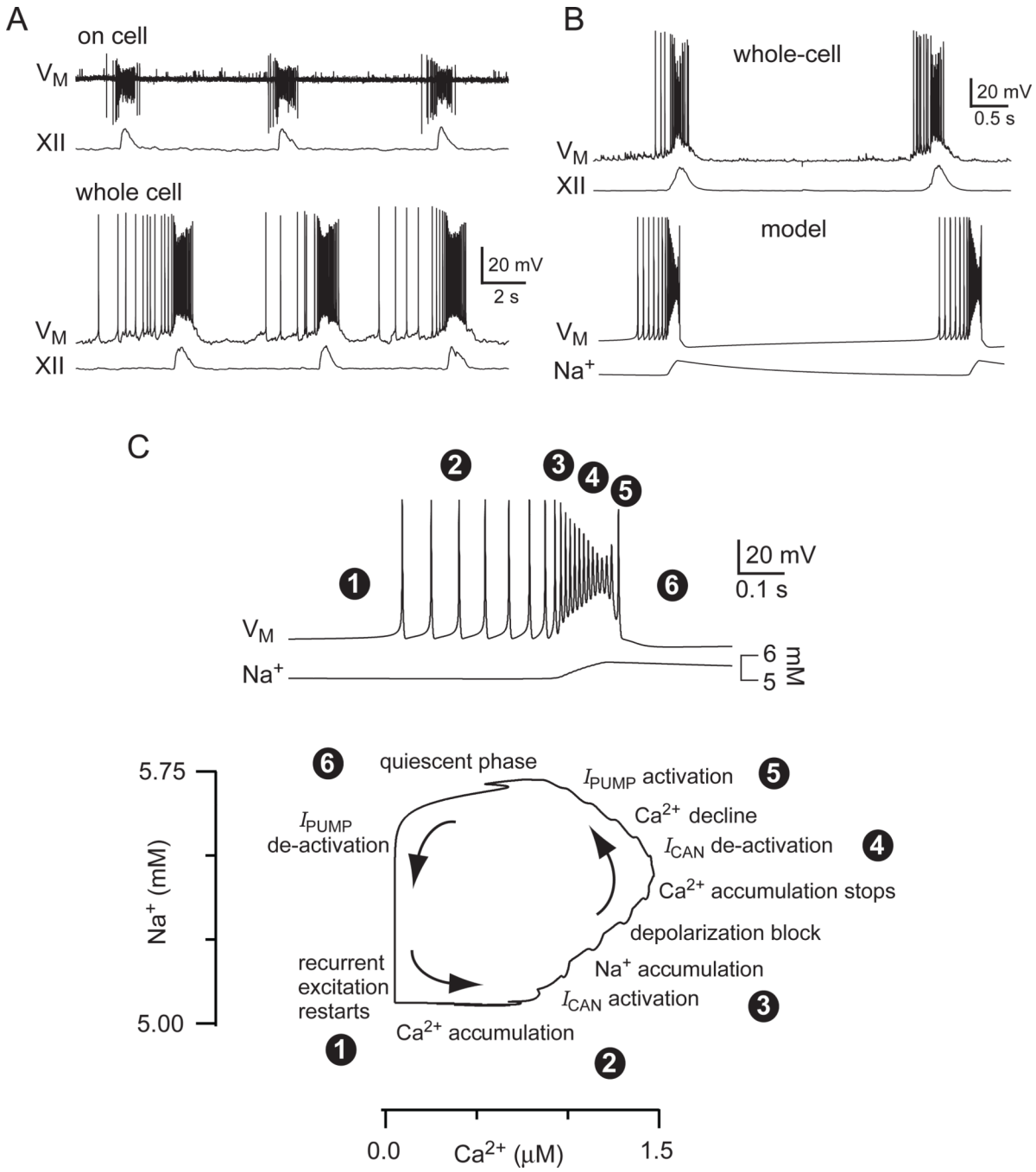

Figure 16.

The group-pacemaker hypothesis realized in an explicit mathematical model. **A**) On-cell patch recording in the preBötC with inspiratory motor discharge (XII). Below, whole-cell recording of the same cell as above after rupture of the patch, also with XII output. Baseline membrane potential was −60 mV. **B**) Data from another preBötC neuron in whole cell recording is plotted with the model behavior. **C**) Fast sweep of a burst in the model from B (above) coded with numerals to illustrate the sequence of physiological steps in one model burst in the Na^+-Ca^{2+} phase plane, which is also displayed. Specific captions are superimposed with the circle-enclosed numbers to encapsulate model dynamics in sequence.

See text for more detail. These data were modified with permission from Rubin *et al.* (2009) Proc Natl Acad Sci USA, 106, 2939–44